45. Environment, Health and Safety Issues in Nanotechnology

Rui Chen, Chunying Chen

With the rapid development of nanotechnology and its application, lots of nanomaterials or nanorelated products are now used in society. Nanotechnology offers substantial economic and societal benefits, but its impacts on environment, health, and safety (EHS) issues are not clearly understood or defined. Interactions between nanomaterials (sourced from nanotechnology development) and the human body and even with the ecological system have attracted much concern. In this chapter, the impacts of the development of nanotechnology on EHS issues has been surveyed focusing on present knowledge of the most important nanomaterials, dominant physicochemical characteristics which contribute to relevant toxicities, and state-of-the-art techniques and established biomarkers within this research field. This information may not be enough to fill the knowledge gap concerning the impacts of nanotechnology on EHS, but should help scientists and authorities to realize the risks involved and to take steps for sustainable development in the foreseeable future.

45.1 Impacts of the Development of Nanotechnology on Environment, Health, and Safety Issues

As illustrated in this handbook, nanotechnology has undergone broad development in terms of the techniques of characterization, fabrication, and manufacturing to keep pace with actual requirements from fields such as electronics, cosmetics, catalysis, gas sensing, energy storage, structural materials, environmental remediation, medical diagnostics, and drug delivery [45.1]. Nanomaterials (NMs) or nanoparticles (NPs) with novel physicochemical properties are the main products or research subjects in nanotechnology development. Among such properties, the most significant change in the properties of NPs is the increase in the surface-to-volume ratio compared to their large bulk counterparts. Importantly, the emergence of these products and research subjects, along with their applications and extinctions has led to great concern over adverse impacts on the environment, health, and safety (EHS). NPs may be released into the environment with the possibility of human or ecosystem exposure at various stages in their life cycles (Fig. 45.1). It is proposed that NPs may enter the body and accumulate in organs, such as lung, liver, spleen, kidneys, or brain, potentially causing harm or death to humans and animals, and the release of NPs into the environment might

B. Bhushan (Ed.), *Springer Handbook of Nanotechnology*, DOI 10.1007/978-3-319-49347-3_45

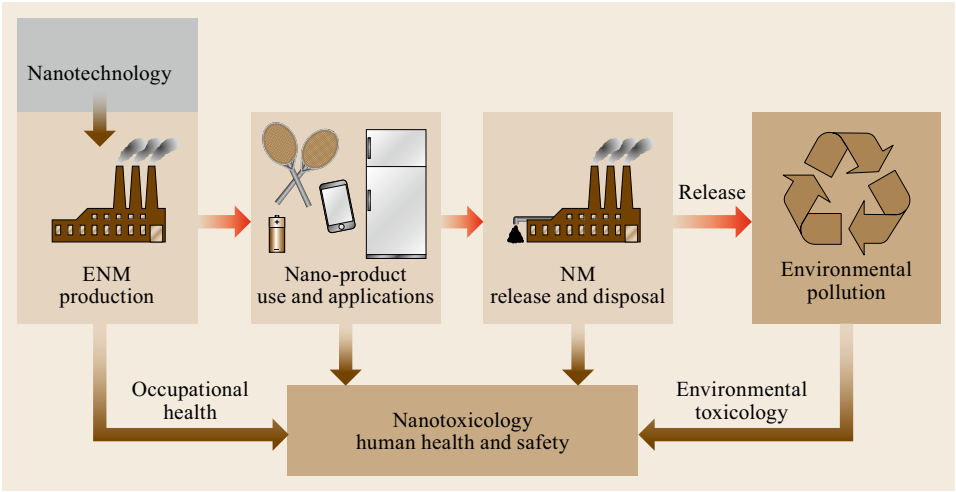

Fig. 45.1 The impacts of the development of nanotechnology on environment, health, and safety (EHS). The *red arrows* show the flows of nanomaterials to the environment: production, use, and disposal of nanoproducts, and release in the environment. The *brown arrows* show the potential health and safety impacts from procedures initiated by the development of nanotechnology

harm the ecological system. Consequently, the field of nanotoxicology emerged around 2004 to 2005 in an attempt to answer critical questions related to these EHS issues [45.2, 3]. *Oberdörster* [45.4] defined nanotoxicology as the study of the adverse effects of engineered nanomaterials (ENMs) on living organisms and the ecosystem, including the prevention and amelioration of such adverse effects. According to a report [45.5] from the Committee to Develop a Research Strategy for Environmental, Health, and Safety Aspects of Engineered Nanomaterials (National Research Council, USA), there are many issues in relation to EHS of NMs:

1. Engineered nanomaterial sources and manufacturing
2. Modifications, fate, and transport
3. Bioavailability and dose
4. Effects on organisms and ecosystems.

As particularly important for EHS, topics related to nanotoxicology and ecotoxicology of NMs will be paid the most attention in this chapter.

NMs/NPs are also defined as nanosized materials/particles that have at least one dimension less than 100 nm. Man-made NMs are generally called engineered nanomaterials (ENMs). Ultrafine particles (UFPs) refers to airborne particulates of less than 100 nm in aerodynamic diameter, i. e., particles generated through the use of nanotechnology, diesel exhaust particles, products of cooking, heating, and wood burning in indoor environments [45.9]. Alongside the booming development of nanotechnology, life-cycle assessment of EHS impacts is important yet difficult to carry out because of the lack of enough detail on the ENMs [45.6]:

1. The manufacturing processes of newly developed NMs are usually evolutional, i. e., with constant changes before final standardization. Thus, EHS impacts could vary considerably among different production procedures.
2. The formula of NMs and related manufacturing processes are new and often subject to confidentiality constraints in the nanotechnology industry.
3. NM release and ecotoxicology impacts are ambiguous at both the nanoproduct use and application stage and at the final disposal and recycling process stage.

This means risk estimations for impacts of NMs on EHS vary from one scenario to another. However, we still need to deepen our understanding of such impacts from the whole life-cycle perspective in order to address uncertainties over possible future outcomes. This may help to bridge the knowledge gap and provide an opportunity to improve the health and safety of scientists, workers, and consumers who work with or use NMs/NM products or are exposed to nanoparticles in society.

The NM production process plays an important role in nanotechnology. This is because a high release potential correlates directly with the mass production process of NMs, generally involving pure and uncombined nanomaterials. Thus, workers in this environment are not only at the forefront of risk due to advancements in nanotechnology, but also their working environments have

Table 45.1 Production/utilization quantities of ten nanomaterials in the world and in Europe (in t/yr). Reproduced with permission from [45.8]

ENMs	Worldwide (t/yr) median and 25/75 percentile	Europe (t/yr) median and 25/75 percentile	US (t/yr) [45.6] range	Switzerland (t/yr) [45.7] in brackets values extrapolated to Europe
TiO_2	3000 (550–5500)	550 (55–3000)	7800–38 000	435 (38 000)[b]
ZnO	550 (55–550)	55 (5.5–28 000)		70 (6100)
SiO_2	5500 (55–55 000)	5500 (55–55 000)		75 (6500)
FeO_x	55 (5.5–5500)	550 (30–5500)		365 (32 000)
AlO_x	55 (55–5500)	550 (0.55–500)		0.005 (0.4)
CeO_x	55 (5.5–550)	55 (0.55–2800)	35–700	
CNT	300 (55–550)	550 (180–550)	55–1101	1 (87)
Fullerenes	0.6 (0.6–5.5)	0.6 (0.6–5.5)	2–80	
Ag	55 (5.5–550)	5.5 (0.6–55)	2.8–20	3.1 (270)
Quantum dots (QDs)	0.6 (0.6–5.5)	0.6 (0.6–5.5)		

[a] The median and the 25/75 percentile are given, rounded to two significant numbers.
[b] The values in brackets for Switzerland were extrapolated using the population of Switzerland (6.9 million) to Europe (593 million)

high priority for the establishment and implementation of responsible practices [45.10]. The basis of evaluation of EHS impacts from nanotechnology is the structure of the ENM life cycle. The first step in NM release assessment is to obtain knowledge of the production process which determines the maximum amount of NMs that could potentially be released to the environment. This means that the most accurate estimation of NMs that could potentially be released to the environment may be the one that is based on the production volume of the raw nanomaterials. In 2012, *Piccinno* et al. [45.8] summarized the production quantities of ten engineered nanomaterials based on their own survey and other literature sources [45.6, 7]. NMs like silica, titania, alumina, iron oxides, and zinc oxides dominate the ENM market in terms of mass flow through the global economy (Table 45.1). Within this list, TiO_2 is by far the most significant ENM in terms of exposure based on modeling estimation [45.11, 12]. The modeling of the NM's flow should generally track its entire life cycle which is illustrated in Fig. 45.1: this includes ENM production, incorporation into products, ENM release from products during use, transport and disposal of ENM during and after recycling processes, transfer to air, soil, water and sediments (ecosphere), and transport within environmental compartments of the nature system. The amounts of ENM in said compartments provides the basis for calculating the overall environmental concentrations of ENM [45.13]. Recently, using dynamic probabilistic material flow modeling, *Sun* et al. [45.14] found that the concentrations of all ENMs in all compartments of the nature system are increasing with the increase of production and applications of ENMs, i. e., of nano-TiO_2, nano-ZnO, nano-Ag, and carbon nanotubes (CNTs) for example, in the world. ENMs generally enter the Earth's surface water first and end up in the sediment where the accumulated concentrations of CNTs and nano-TiO_2 were estimated to be 6.7 μg/kg (CNTs) and about 40 mg/kg (nano-TiO_2) in the worst-case scenario [45.14]. The concentration of NMs in the nature system is a crucial factor in the evaluation of EHS impacts. However, one report shows that Ag ENM contributed to a higher ecotoxicity to freshwater algae, daphnia, and fish compared to TiO_2 ENMs, even though a much lower concentration had accumulated in the ecosystem [45.15].

In nanotechnology there are two principle nanoscale manufacturing strategies: the top-down and the bottom-up approach [45.16]. The top-down approach begins at the bulk level and involves miniaturization to nanoscale dimensions via carving or grinding methods, i. e., lithography, etching, or milling. The bottom-up approaches begin at the atomic or molecular level with growth through nucleation and/or growth from liquid, solid, or gas precursors via chemical reactions or physical processes, i. e., through techniques like sol-gel or epitaxy [45.16, 17]. The top-down approach dominates compared to the bottom-up approach, but it is believed to produce more waste. It has been suggested that the bottom-up approach represents should be emphasized in order to minimizing the unwanted waste for sustainable development in nanotechnology [45.17].

The release of NMs during production and manufacturing not only constitute a possible release pathway to the environment, but also has high relevance in regard to occupational exposure. With no release and no exposure there will be no impact on EHS. Actually, from a life-cycle viewpoint there is significant impact from

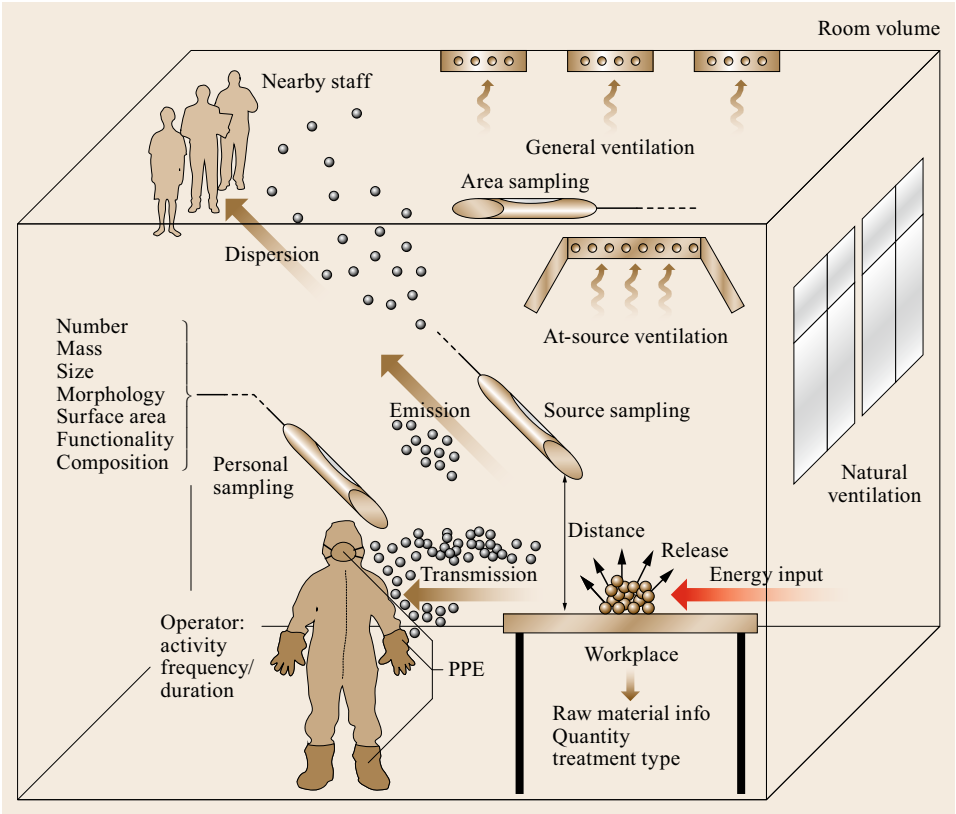

Fig. 45.2 Diagram representing various elements and processes in an occupational exposure scenario. Reproduced with permission from [45.18]

the process of NM production. Figure 45.2 shows a typical occupational NM-handling setting where ENMs could be released, emitted, and transported, resulting in actual exposure to workers [45.18]. Exposure assessment and management are critical in order to minimize impacts on the production environment, although there are too many variants in application situations. Detailed procedures and strategies for occupational exposure assessment and risk evaluation can be found in the literature [45.10, 18]. Further, appropriate risk management practices including engineering control systems in working environments or personal protective equipment (PPE) for individuals are important but beyond the scope of this chapter. In addition, it would be informative if more effort is paid in the future to evaluations of impacts during use and application processes, and the final disposal of nanorelated products.

45.2 Current Progress of the Most Important Nanomaterials

45.2.1 Carbon Nanotubes

Much of the concern associated with nanotechnology comes from the potential risks of CNTs [45.19, 20]. Typically a few nanometers in diameter, CNTs are long and thin cylinders of carbon with a single wall or multiple walls defined as single-walled carbon nanotubes (SWCNTs) and multiwalled carbon nanotubes (MWCNTs), respectively. They have a needle-like shape and are strong and tough in character, similar to asbestos. In vitro evidence showed that exposure to CNTs could reduce viability, induce apoptosis, and cause DNA (deoxyribonucleic acid) damage [45.23, 24]. These adverse effects may result from the interruption of cellular redox status after CNT exposure, e.g., increasing ROS (reactive oxygen species) and malondialdehyde (MDA) levels, as well as altering superoxide dismutase (SOD) activity and glutathione peroxidase (GSH-Px) levels as previously reported [45.25–27]. In vitro studies based on mammalian cell models often show inconsistent results because of the different cell lines, doses, and exposure times used. However, in vivo pulmonary tox-

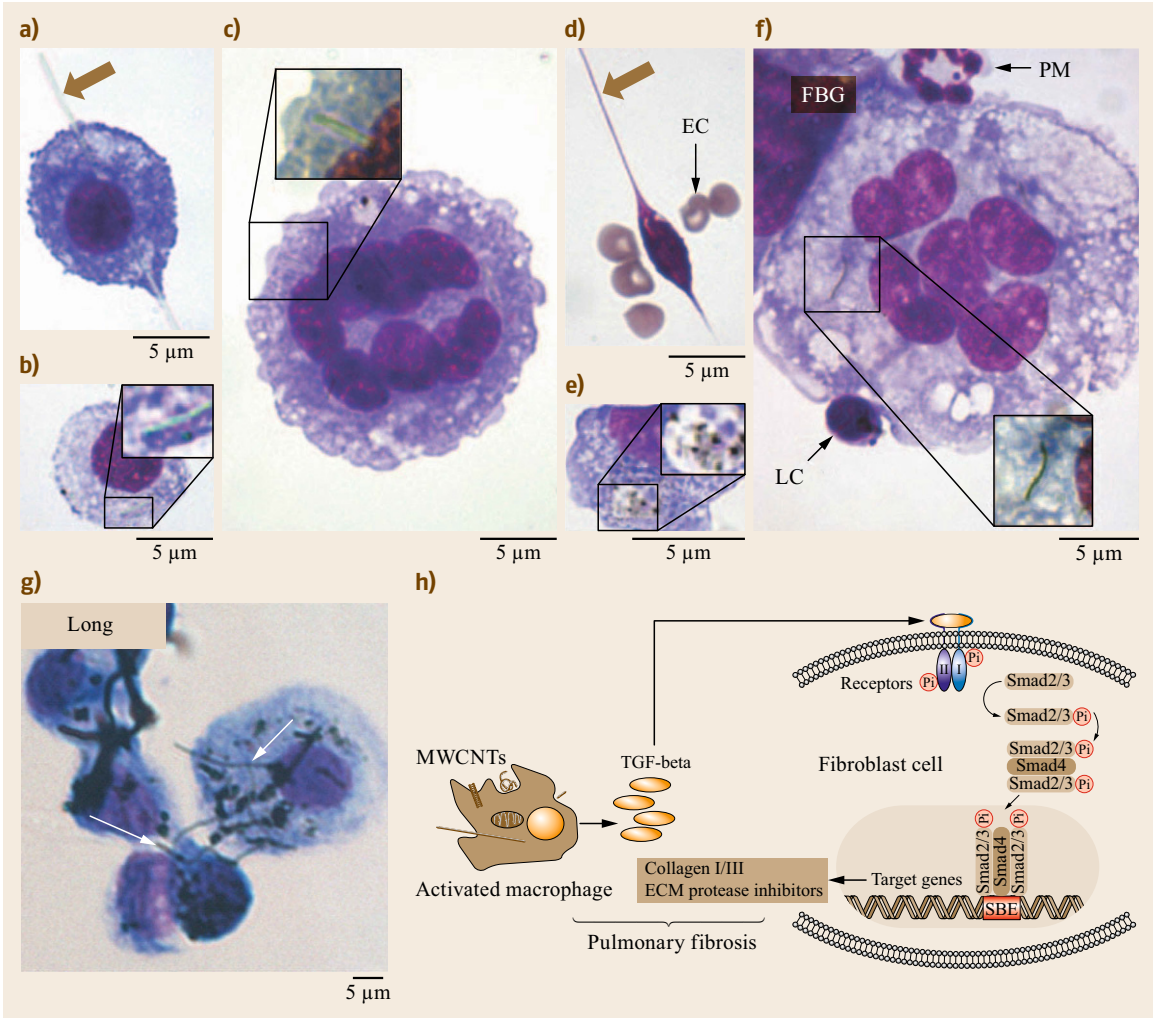

Fig. 45.3a–h The phagocytosis of asbestos and CNTs by macrophages. **(a,b)** Histological sections show incorporation of long-fiber amosite **(a)** (*arrow*) leading to *frustrated phagocytosis*, but short-fiber amosite **(b)** (see *inset*) is successfully phagocytosed by peritoneal macrophages. **(c)** Representative image of a foreign body giant cell after injection of long-fiber amosite containing short fiber fragments. **(d)** Like long-fiber amosite, long CNTs (> 15 µm) also lead to frustrated phagocytosis in peritoneal macrophages (EC, erythrocytes). **(e)** In contrast, short CNTs (< 5 µm) can be readily phagocytosed (see *inset*). **(f)** Foreign body giant cells (FBGC) are also present after injection of long CNTs in peritoneal macrophages (see *inset* for internalized fibers) (PMN, polymorphonuclear leukocyte; LC, lymphocyte). **(g)** Representative optical microscope image to show the in vivo cellular uptake of MWCNTs by alveolar macrophages. **(h)** MWCNTs promote pulmonary fibrosis through the TGF-β/small mothers against decapentaplegic (Smad) signaling pathway. All images are shown at ×1000 magnification with a 5 µm scale bar (after [45.21], **(g,h)** from [45.22] reprinted with permission)

icity studies usually show CNT causing clear adverse toxicity effects. It has been found in animal experiments that exposure to long CNTs (longer than 15 µm) at the mesothelial lining of the body cavity of mice will result in asbestos-like, length-dependent, pathogenic behaviors including inflammation and granulomas [45.21]. The macrophages at the mesothelial lining may resort to *frustrated phagocytosis* and giant cell formation caused by macrophage fusion in inflammatory conditions when attempting to phagocytose or engulf long CNTs (Fig. 45.3a–f). These results suggest a potential link between inhalation exposure to long CNTs and mesothelioma which is generally regarded as the specific type of cancer caused by inhalation exposure to

asbestos, although it remains unknown whether there will be sufficient exposure in the environment or workplace to actually cause it.

Granuloma formation and/or fibrotic responses in the lungs are the dominant injuries after inhalation exposure to CNTs. It is worth noting that long CNTs have much more significant effects [45.22, 28]. The underlying mechanisms were systematically investigated in our lab. The alveolar macrophages show the same *frustrated phagocytosis* phenomenon with peritoneal macrophages when phagocytosing long MWCNTs (Fig. 45.3g). It was found that TGF (transforming growth factor)-β1 could be induced in alveolar macrophages or released from the bronchiolar epithelium by MWCNT exposure, which plays an important role in MWCNT-caused pulmonary fibrosis (Fig. 45.3h). At the same time, the fibroblast-specific protein-1, α-smooth muscle actin, and collagen III were significantly upregulated by the induction of TGF-β1 [45.22]. Further research showed TGF-β1 secreted from macrophages serves as a critical paracrine stimuli to fibroblasts by directly activating TGF-β/small mothers against decapentaplegic homolog 2 (Smad2) signaling in fibroblasts or epithelial cells. This stimulation then induces the fibroblast-to-myofibroblast transition and epithelial–mesenchymal transition (EMT), respectively, both of which contribute to CNT-induced fibrotic responses [45.28].

The inhalation of carbon nanotubes has a high possibility to induce pulmonary fibrosis but also can directly cause acute and serious injuries to the pulmonary system [45.30, 31]. In our research, we tested the pulmonary toxicity of SWCNTs by intranasally instilling exposure using the spontaneously hypertensive rat model [45.32]. The inflammation, oxidative stress, and cell damage levels in the bronchoalveolar lavage fluid (BALF) were significantly increased at 24 h postexposure. The increased endothelin-1 in BALF and plasma and angiotensin I-converting enzyme in plasma suggested endothelial dysfunction in the pulmonary circulation and peripheral vascular thrombosis. Histological data on lung tissues showed that SWCNT-laden macrophages move to centrilobular locations and form multifocal pulmonary granuloma [45.32]. The formation of pulmonary granuloma lesions were the result of the lungs' immune response to the foreign substances that can not easily be eliminated [45.33, 34]. Further, the subchronic toxic effects and cardiovascular effects of CNTs were disclosed at 7 and 30 days postexposure to the inhalation system in rats [45.35]. These results suggest that respiratory exposure to CNTs not only induces acute pulmonary toxicity but also poses long-term adverse effects on the whole cardiovascular system. Humans with existing cardiovascular diseases are also susceptible to CNT exposure.

Knowledge of biodistribution and biopersistence in the body can help better understand the potential effects of their exposure to humans. Using the Raman spectroscopy mapping method it has been found that inhaled CNTs have the ability to penetrate deep into the lungs, cross the pulmonary epithelium, and enter the bloodstream [45.36]. Then, the extrapulmonary transport of CNTs was disclosed after inhalation exposure in C57BL/6 J mice by testing at 5 h/day for 12 days with a concentration of 5 mg/m^3 in a whole-body inhalation system [45.29]. It has been shown that inhaled MWCNTs, which were deposited in the lung, were transported to the parietal pleura, the respiratory musculature, liver, kidney, and heart in a singlet form and accumulated even until day 336 postexposure (Fig. 45.4). Similar biodistribution evidence for CNTs in liver, kidneys, and spleen has been reported after exposure to MWCNTs in rats using the inhalation system [45.35, 37]. After entering the blood circulation, CNTs will interact with blood proteins, i. e., fibrinogen (BFg), immunoglobulin, albumin, transferrin (Tf), and ferritin. Indications showed that there was a competitive binding of different blood proteins onto the surface of SWCNTs, which was governed by each protein's unique structure and the amount of hydrophobic residues of each kind of protein (Fig. 45.5). Atomic force microscopy (AFM) images indicated that the adsorption of transferrin and BSA (bovine serum albumin) quickly reached thermodynamic equilibrium at about 10 min, while fibrinogen and gamma-globulin (γ-Ig) gradually packed onto the SWCNT surface in a much longer period of about 5 h. Both fluorescence spectroscopy and SDS-PAGE have shown surprising competitive adsorptions among all the blood proteins examined, with the competitive order: BFg > γ-Ig > Tf > BSA. The far-UV circular dichroism (CD) spectra observation shows that the protein secondary structure has greatly changed for BFg and γ-Ig, with a decrease in the α-helical content and an increase in the β-sheet structure (Fig. 45.5g). In addition, our molecular dynamics simulations of SWCNTs binding with BFg, BSA, γ-Ig, and Tf complexes showed that both the contact residue numbers and binding surface areas exhibited the same sequence order: BFg > γ-Ig > Tf > BSA, in agreement with the experimental findings. Further analysis showed that the π–π stacking interactions between SWCNTs and aromatic residues (Trp, Phe, and Tyr) play a critical role in their binding capabilities. These different protein-coated SWCNTs may have different cytotoxicity by influencing the subsequent cellular responses [45.38].

The knowledge on the ADME (absorption, distribution, metabolism and excretion) of NMs could give help on the understanding of their adverse impacts to EHS. Much more research efforts should be taken

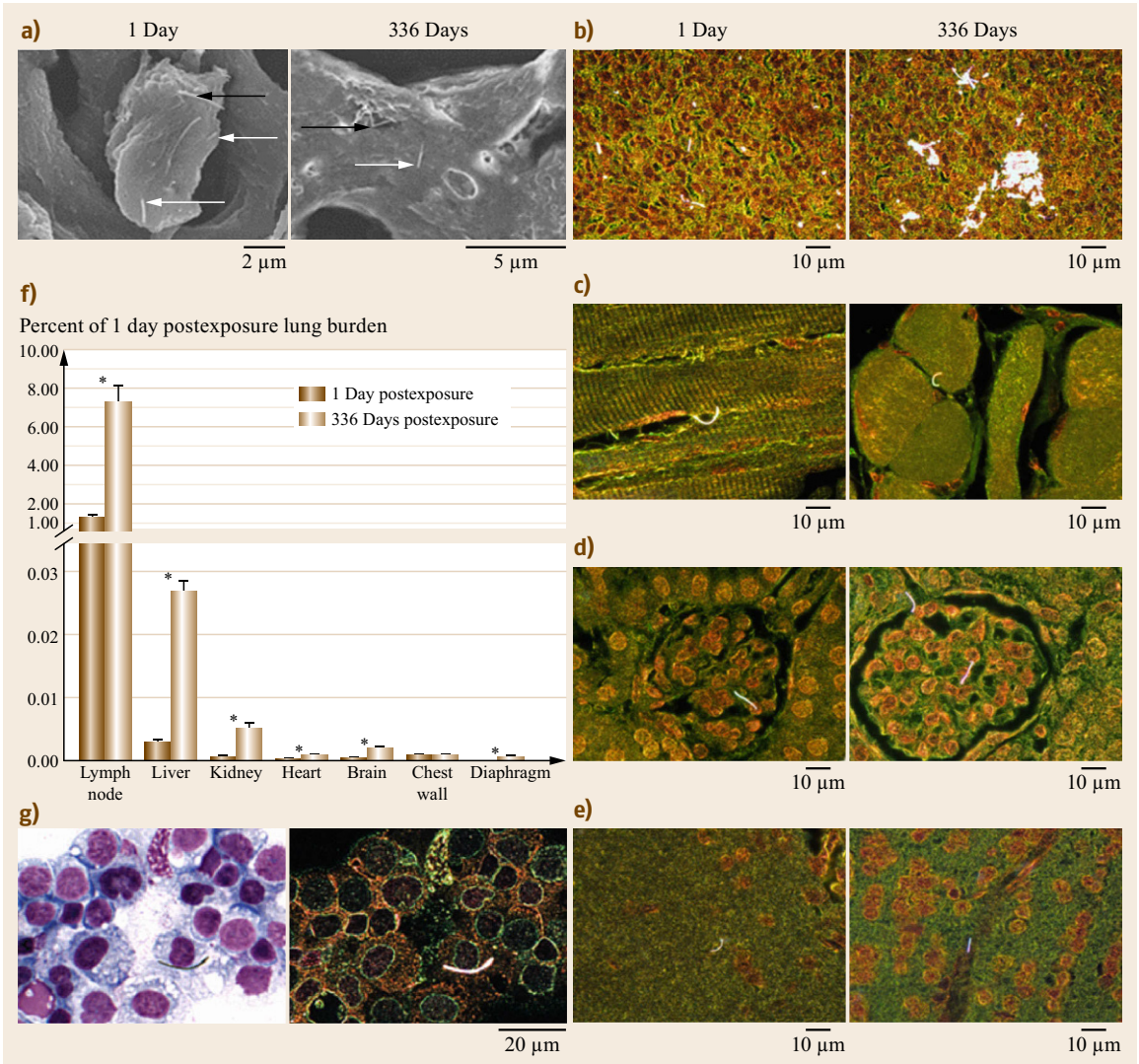

Fig. 45.4a–g Extrapulmonary biodistribution of CNTs after inhalation exposure. **(a)** Field-emission scanning electron microscopy (FESEM) images of alveolar macrophages 1 and 336 days postexposure. *Arrows* show the typical examples of MWCNT fibers protruding from the surface of alveolar macrophages (*black arrow* multiple fibers, *white arrows* singlets). **(b–e)** Enhanced dark-field images of tissue sections 1 and 336 days after CNT inhalation exposure. Tissues are from tracheobronchial lymph nodes, diaphragm, kidney and brain, respectively. **(f)** Percentage of 1 day postexposure lung burden detected in tracheobronchial lymph nodes, extrapulmonary organs, diaphragm, and chest wall. By 336 days postexposure there was a 7-fold increase in MWCNT in extrapulmonary organs and diaphragm over that measured at 1 day postexposure. Categories of extrapulmonary organs are ordered relative to MWCNT concentration in the respective tissue. *Asterisks* indicate significant difference between day 1 and 336 days postexposure values, $P < 0.05$. **(g)** Light and enhanced dark-field micrographs of MWCNTs detected in lavage of pleural space. The figure shows a comparison of the light and enhanced dark-field image of a singlet MWCNT in lavage of the pleural space in mice at 336 days postexposure (after [45.29])

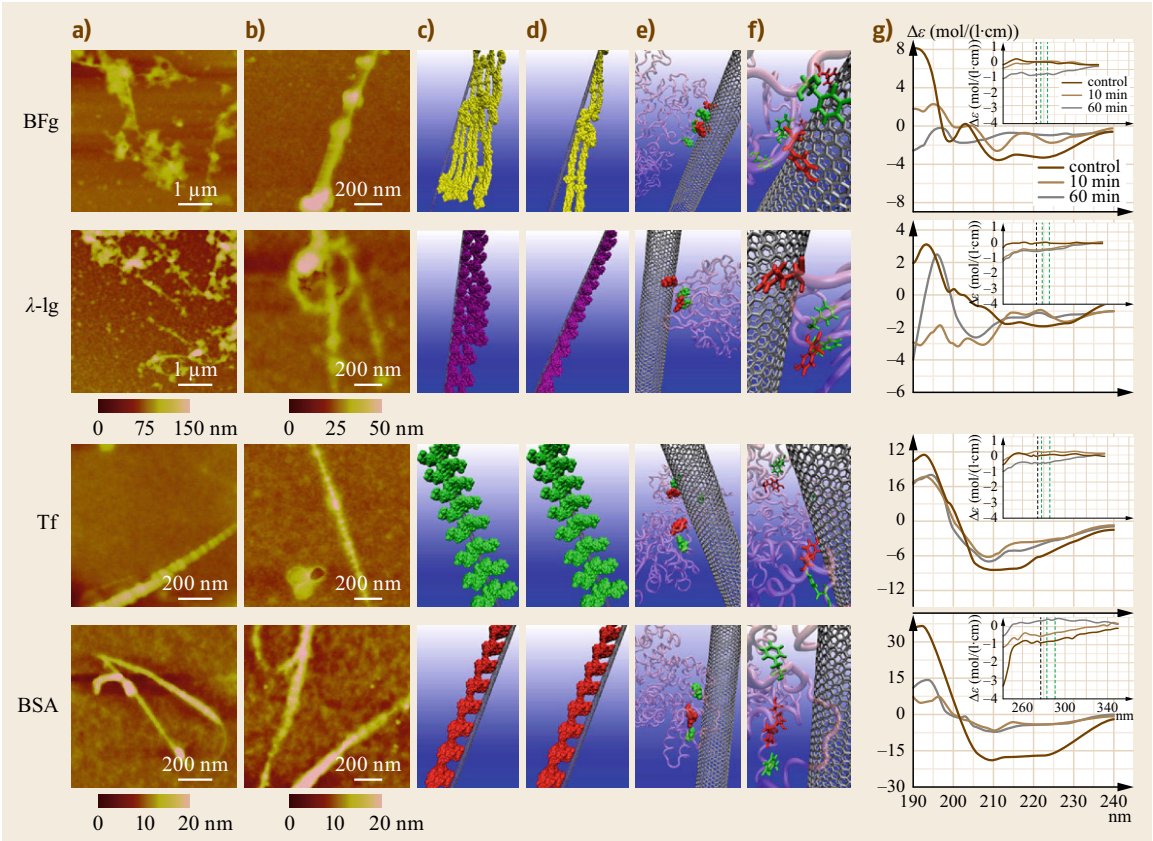

Fig. 45.5a–g The interactions between SWCNTs and human blood proteins (BFg, γ-Ig, Tf, BSA). AFM images of proteins after incubation with SWCNTs for 10 min **(a)** and 5 h **(b)**. Molecular modeling illustrations for proteins (bead representations) binding to SWCNTs after incubation for 10 min **(c)** and 5 h **(d)**. **(e)** Locations of the most preferred binding sites on proteins for SWCNTs. Residues highlighted in van der Waals representation corresponding to tyrosine in *red* and phenylalanine in *green*. Other protein parts are presented in *transparent pink* with the new cartoon drawing method. **(f)** The detailed orientations of aromatic rings of tyrosine and phenylalanine residues interacted to six-member rings of SWCNTs colored in *silver*. The tyrosine residues are rendered as Licorice representations and shown in *red*, with phenylalanine residues are in *green*. **(g)** The far-UV circular dichroism (CD) spectra of proteins after incubation with SWCNTs and the insets are near-UV CD spectra of proteins incubated with SWCNTs (after [45.38])

on this topic for CNTs. Other carbon NMs including fullerene and derivatives, graphene, and graphene oxide have a lower production quantity compared with CNTs (Table 45.1). Even so, a cautious attitude should be taken with all these carbon nanomaterials [45.40]. More information and data on the impact of these carbon NMs on EHS are urgently needed to support future effective assessment.

Fig. 45.6a–g Cytotoxicity and genotoxicity analysis of BSA-coated AgNPs in the cell line CHO-K1. TEM (transmission electron microscope) images of CHO-K1 cells when treated with 10 µg/ml of AgNPs for 6 h **(a)** and 24 h **(b)**. For cells treated with AgNPs and Ag^+, shown in the figure are changes in mitochondrial activity **(c)** by CCK-8 assay and intracellular ROS levels **(d)** that were labeled by DCFH-DA fluorescence density and determined by flow cytometry. DNA adducts induced by AgNPs and Ag^+ after 24 h exposure **(e)**. Methylmethanesulfonate (MMS) was used as a positive control. DNA oxidative adduct, 8-hydroxydeoxyguanosine (8-OxodG), which can be induced by AgNPs and Ag^+ after 24 h exposure **(f)**. Fluorescence microscopic images of micronuclei induced by AgNPs and Ag^+ after 24 h exposure **(g)**. Statistically significant difference from control is expressed as $*(P < 0.05)$ and significant difference between AgNPs and Ag^+ for the same amount of silver is expressed as $\dagger(P < 0.05)$. Reproduced with permission from Elsevier [45.39] ►

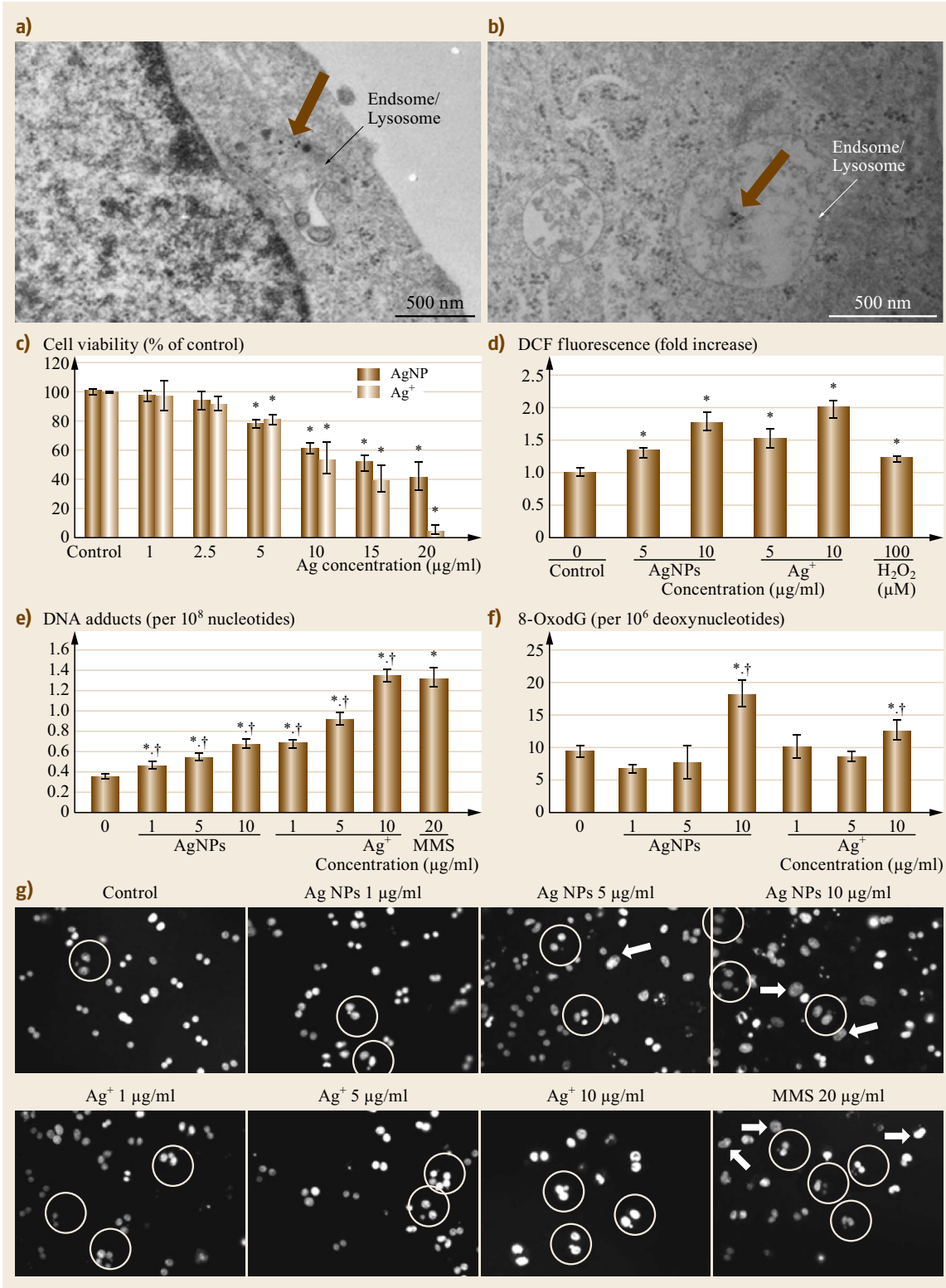
a)
Endsome/
Lysosome
500 nm
b)
Endsome/
Lysosome
500 nm
c) Cell viability (% of control)
AgNP
Ag+
Control
Ag concentration (µg/ml)
d) DCF fluorescence (fold increase)
Control
AgNPs
Ag+
H2O2
(µM)
Concentration (µg/ml)
e) DNA adducts (per 10^8 nucleotides)
AgNPs
Ag+
MMS
Concentration (µg/ml)
f) 8-OxodG (per 10^6 deoxynucleotides)
AgNPs
Ag+
Concentration (µg/ml)
g)
Control
Ag NPs 1 µg/ml
Ag NPs 5 µg/ml
Ag NPs 10 µg/ml
Ag+ 1 µg/ml
Ag+ 5 µg/ml
Ag+ 10 µg/ml
MMS 20 µg/ml

45.2.2 Silver Nanoparticles

With excellent antimicrobial activity, silver nanoparticles (AgNPs) are widely used as a major ingredient in industrial, consumer, and medical products [45.41, 42]. For example, AgNP-related products have been used in consumer products such as surface cleaners, room sprays, toys, antimicrobial paints, home appliances, food storage containers, textiles, and medical products including wound dressings, surgical instruments, urinary catheters, and bone prostheses. Several investigations have shown that silver-containing textiles could release significant amounts of Ag into the washing liquid when laundering fabrics [45.43–46]. It is inevitable that these discharged silver ions or silver nanoparticles are released into the ecosystem through sewer systems and constitute a high impact on EHS [45.47]. It has been discerned that Ag mostly transforms and precipitates to silver-containing particles like Ag_2S or AgCl during handling or disposal processes [45.46, 48]. Further, recent studies revealed that the reduction of Ag^+ in natural waters can form AgNPs naturally via the mediation of dissolved organic matter or sunlight [45.49–51]. This means that silver has complex transformation mechanisms in the environment [45.52].

As release from source products is inevitable, there is a high possibility that AgNPs will enter the human body and distribute within the circulation system or the organs after exposure. It has been shown that AgNPs are captured by the reticuloendothelial system and quickly distributed to other tissues after entering the blood [45.53–56]. In detail, AgNPs were mostly distributed to the liver, spleen, lung, and kidneys, and much less to the brain, heart, and testes after *i.v.* exposure [45.57, 58]. Interestingly, the concentrations of Ag in the blood remains steady with a slightly decreasing trend till at least 14 days for a single i.v. injection of AgNP, which means that AgNPs may be degraded and removed in a time-dependent manner [45.59]. The kinetic distributions of AgNPs in the body are important because they determine relevant toxicity. However, the mechanism of AgNP toxicity has not been clearly defined. Currently, there are three hypotheses to explain the toxicity of AgNPs after exposure. First, the ions released from NPs contribute to their toxicity. Second, the toxicity is caused through a silver ion-independent mechanism. Third, the Ag ions released from the endocytosed AgNPs in the cell dominate the toxicities, and this generally happens at endosome or lysosome locations. In reality, a combination of these may lead to the AgNP toxicity mechanism. *Jiang* et al. [45.39] showed that AgNPs were mostly localized in the endosome/lysosome in Chinese hamster ovary (CHO-K1) cells after exposure (Fig. 45.6a,b). Then, the cytotoxicity and genotoxicity of BSA-coated AgNPs on CHO-K1 were investigated. This showed that both BSA-AgNPs alone and Ag ions can up-regulate the cellular ROS level with the production of oxidative adducts, 8-hydroxydeoxyguanosine (8-OxodG), and induce the formation of micronuclei (Fig. 45.6c–f). The genotoxicity of AgNPs is prominent within the induced adverse outcomes, and merit special attention in future [45.60, 61]. Further research in our lab showed that there is a high possibility that AgNPs will cause adverse effects by the third mechanism listed above. Evidence concerning the intracellular fate of AgNPs is derived using x-ray absorption near-edge structure (XANES) spectroscopy, which is used to study the degradation and biointeraction of nanoparticles in biological systems [45.62, 63]. About 14.2% of the internalized silver was oxidized to Ag−O− after 12 h incubation of AgNPs in the CHO-K1 cell line. While 61.5% of the silver was present as Ag−S− after 24 h, suggesting that binding of Ag to sulfide groups of amino acids and proteins may be involved in the dissolution process of AgNPs. This intracellular binding of silver ions to proteins disrupts protein structure and function, thereby resulting in toxic effects [45.64].

The surface charge and various surface coatings of AgNPs play an important role in in vivo and in vitro toxicity, biodistribution, and pharmacokinetics [45.65]. Branched polyethyleneimine (BPEI)-coated AgNPs led to the highest toxicity in cells and mice, while the nearly neutral polyethylene glycol (PEG)-coated AgNPs showed low toxicity and long half-life in blood, indicating a high potential for application in medical products [45.65]. This means that the safety of silver NMs can be improved by adoption of particular surface coating strategies in their application [45.66–68]. Improving our understanding of the toxicity mechanisms of AgNPs could help with their safety evaluation and potential risks to EHS, and from different aspects such understanding may contribute to facilitating the design of safer and more effective antimicrobial products in the future.

45.2.3 Zinc Oxide Nanoparticles

Zinc oxide NPs have been used in personal care products including cosmetics and sunscreens as they efficiently absorb ultraviolet radiation and are also highly transparent to visible light. Attracting great concern are potential impacts through human exposure and health impacts at each stage of their manufacture and use [45.69, 70]. Dermal penetration is the first step in evaluating the toxic impacts of ZnO NPs on humans in regard to their long-term skin retention character.

Gulson et al. [45.71] tested the penetration efficiency of ZnO NPs by focusing on ^{68}Zn from enriched ^{68}Zn particles in sunscreens. Small amounts of ^{68}Zn tracer were tested in the blood of 20 human volunteers who received twice daily applications over 5 days. The highest ^{68}Zn concentrations were found in females after exposure to the ^{68}Zn nanoparticles [45.71]. This means that long-term retention of NMs on the skin may lead to dermal penetration by outer particles, although usually at the trace amounts level. For damaged skin, exposure of epidermal and dermal cells to high concentrations of ZnO NPs is sure to cause cytotoxicity and undesirable immune responses, which will instigate the penetration of even more particles to even deeper sites or even into the lymphatic or blood circulation [45.70, 72].

Inhalation exposure to ZnO fumes in the working environment can affect normal bodily functions, for example by causing metal fume fever, which is characterized in humans by short-term pulmonary and systemic alterations and is caused by inhalation of metal oxide aerosol [45.73]. It has been reported that humans exposed to ZnO particle fumes (MMD 300 nm) at 2.5 mg/m^3 for 2 h developed symptoms of metal fume fever with a significant increase of cytokine interleukin (IL)-6 in peripheral blood [45.74]. Human clinical experimental study showed that inhalation exposure of ZnO fumes for 10 to 30 min at a high concentration of 20–42 mg/m^3 increased the number of proinflammatory cytokines and neutrophils in BALF [45.75]. Animal experiments illustrated that inhalation of relatively lower concentrations of ZnO NPs, 1.1 to 4.9 mg/m^3 with occupationally relevancy for 2 week, can generate similar inflammation outcomes in the BALF in rats [45.76]. The National Institute for Occupational Safety and Health (NIOSH) recommended the permissible exposure limit of 5 mg/m^3 averaged over a work shift of up to 10 h/day, 40 h/week for zinc oxide fume inhalation exposure (NIOSH, publication number 0675). Whereas no exposure limit is available for nano-ZnO aerosol to date.

Both in vitro and in vivo systems illustrated that mechanisms underlying ZnO NP toxicity similarly include generation of ROS and subsequent DNA damage and apoptosis [45.77–79]. Oxidative stress produces *free radicals* and has been implicated in various adverse outcomes. For example, *Sharma* et al. [45.80] showed that significant DNA damage in a human epidermal cell line (A431) occurred upon ZnO NP exposure for 6 h at relatively higher concentrations (0.8 mg/ml to 5 mg/ml), while oxidative stress was induced at lower concentrations (0.008–0.8 mg/ml). Zinc ions released from the NPs serve as another key determinant for the toxicity of ZnO NPs [45.81]. Previous research showed that surface coating can considerably mitigate the cytotoxic potential of ZnO NPs by inhibiting ion release and/or minimizing ROS production, i. e., silica shell [45.82] and PEGylation [45.83]. In our own recent research, we found preincubation of ZnO NPs in a supplemented cell culture medium for 24 h could form a hard protein corona on the NP surface. These precoated stable protein layers on the NP surface facilitated further protein adsorption during the cell culture process. The amount of proteins adsorbed on precoated NPs could inhibit both ROS generation and ZnO dissolution and result in lower cytotoxicity [45.84]. This finding demonstrates an effective and convenient way to achieve safe biomedical and environmental applications of ZnO NPs. Besides surface coating, particle size, aspect ratio, doping type, and doping concentration all contribute to their toxicities [45.85]. Quantitative structure–activity relationships (QSAR) modeling is a powerful tool to predict how these physicochemical properties affect the toxicities of ZnO NPs [45.86]. Thus, there is a high chance of developing applicable models to guide the design and optimization of ZnO NPs with safe characteristics in terms of EHS issues.

45.3 Physicochemical Characteristics of Nanoparticles that Determine the Toxicity Impacts

Conventional toxicology places emphasis on chemical composition, dose, and exposure route as the primary variants in toxicity assessment of a chemical or a bulk material. However, many other factors, especially the physicochemical characteristics of nanoparticles, should be considered when we perform the same work in nanotoxicology (Fig. 45.7) [45.87]. This makes nanotoxicity evaluation much more complex and difficult than conventional toxicology [45.88]. There are two types of toxicity-related variants: intrinsic factors such as nanostructure, size, aggregation state etc. as listed in the right column of Table 45.2, and extrinsic factors, such as dose (presented by the metrics of mass/surface area/particle number), cell-/organ-specific responsiveness, exposure routes (e.g., pulmonary exposure, dermal exposure, oral gavage, ocular exposure, intravenous/intradermal/intramuscular/subcutaneous/intraperitoneal administrations), and biological species (e.g., rat, mouse, *Caenorhabditis elegans*, zebrafish, etc.) [45.87]. Understanding the func-

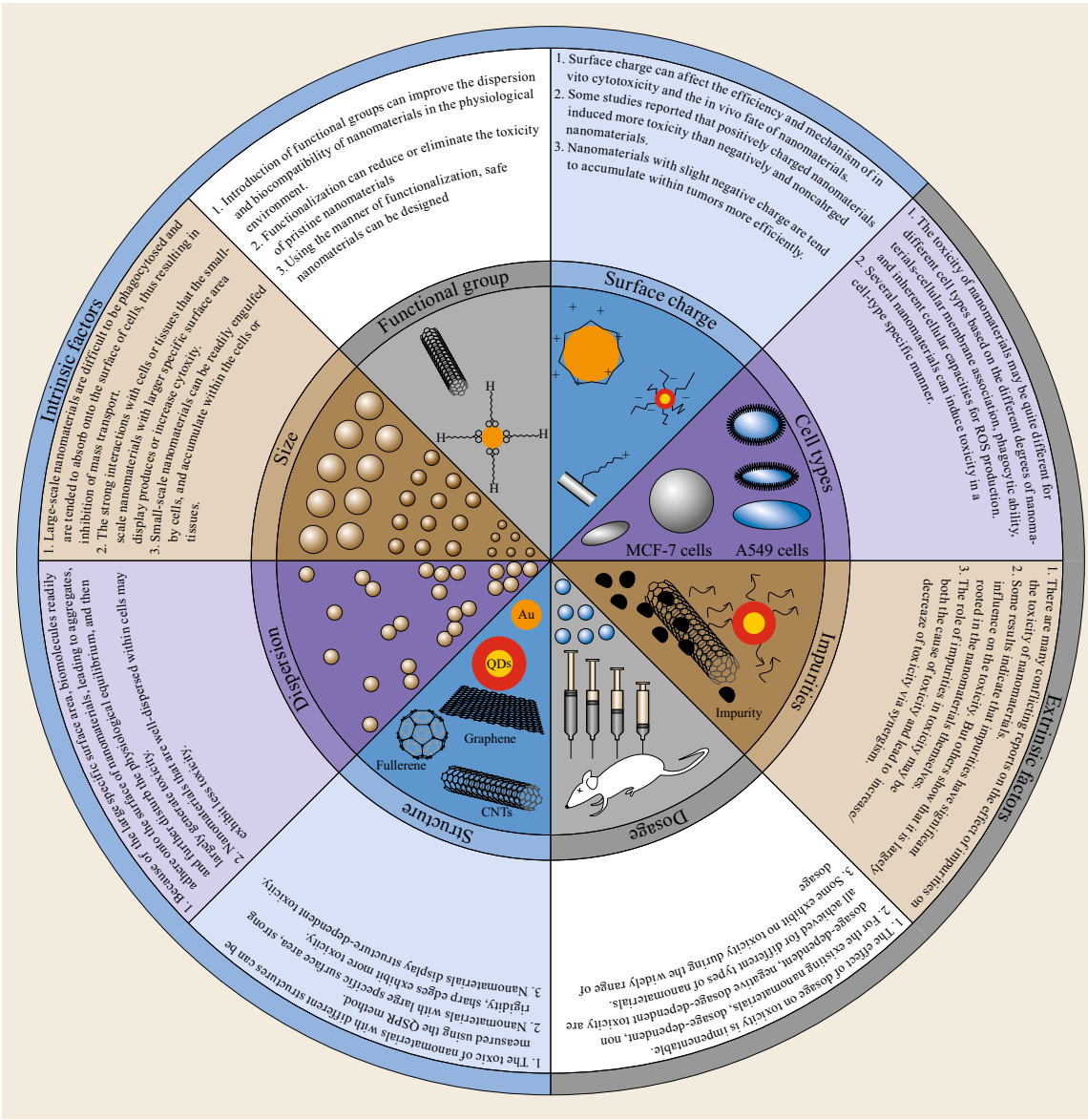

Fig. 45.7 Dominant factors influencing the toxicities of nanomaterials. They are classified into two categories: the intrinsic factors that mostly arise from the physicochemical properties of engineered nanoparticles (ENPs), and the extrinsic factors that include all other factors that can influence the toxic responses of NMs in experimental study or nanosafety assessment during real exposure scenarios (after [45.87])

tions of various physicochemical characteristics of NPs would facilitate the intended design of products with minimized EHS impacts in the future.

45.3.1 Particle Size and Surface Area

Particle size is a critical parameter in NM EHS impacts, which generally leads to the arising of other intrinsic factors. Particle size usually refers to the individual particle, not the agglomeration or aggregated ones which form during production, application, release, and disposal processes. As NM size decreases, the surface area/mass ratio exponentially increases and more atoms are displayed on the particle surface compared with the bulk material. The decreased particle size and increased surface areas make the NM surfaces more reactive to the surrounding biological components. Therefore, chemical reactions including catalytic

Table 45.2 Comparison of the physicochemical characteristics that dominate the toxic responses of nanomaterials with the bulk materials

Bulk material or nanomaterials	Nanomaterials
Chemical composition	Nanostructure (shape, crystal forms)
Particle mass concentration	Particle size/distribution
Reactivity	Particle number
Conductivity	Aggregation/agglomeration
Morphology (crystalline, amorphous, shape, etc.)	Degree and state of dispersion Zeta potential
Physical form (solid, aerosol, suspension, etc.)	Quantum effects Surface area
Purity/Impurities	Surface charge
Surface modification	Surface coating and chemistry
Solubility	Surface structure, crystal face
	Surface adsorbability
	Self-assembly
	...

reactions and redox reactions may occur at the surface of NPs causing the formation of ROS (such as superoxide anions or hydrogen peroxide) and subsequently oxidizing other interacting biomolecules. Many studies have indicated that a small size can increase toxic effects compared to the bulk counterpart [45.89–92]. The particle size influences cellular uptake in vitro, i. e., large latex spheres (>200 nm) had a slower uptake and processing ability compared to smaller ones (50 and 100 nm) [45.93]. In a well-known in vivo study example, inhalation of ultrafine TiO_2 particles (20 nm diameter, 12 week) showed significantly prolonged retention and more inflammation in lung than the inhalation of fine TiO_2 particles (250 nm diameter, 12 week) [45.94]. This means that the physicochemical characteristics of size and surface area have dominant roles in determining toxic potential when NPs interact with organisms.

45.3.2 Nanostructure and Shape

Engineered nanoparticles (ENPs) may exhibit various shapes and structures, e.g., spheres, needles, tubes, rods, etc. For example, CNTs exist as either SWCNTs which are graphite sheets rolled to form a seamless cylinder, or MWCNTs that have many cylinders stacked one inside the other. Similar to CNTs, fullerenes are carbon allotropes composed entirely of carbon, but they are different in form, e.g., hollow sphere, ellipsoid. One representative fullerene is C_{60}. CNTs and fullerenes have various uses based on their novel physicochemical characteristics, e.g., in the biomedical field of bioimaging and therapy [45.95]. However, typically they have poor solubility and are difficult to manipulate in solvents or physiological solutions like serum, which influences their toxicity, metabolism kinetics, and biomedical functions [45.23]. One in vitro study showed that SWCNTs, MWCNTs, and C_{60} exhibit quite different cytotoxicity to alveolar macrophages, although they all represent carbon materials (Fig. 45.8). The comparative toxicities illustrated the following sequence on a mass basis: SWCNTs > MWCNT (with diameters ranging from 10 to 20 nm) > C_{60} [45.96]. CNTs with different lengths contribute to obviously different lung fibrosis potential after inhalation exposure [45.28]. Further evidence showed that short-length MWCNTs not only had lower toxicity but also higher cellular uptake and more obvious removal ability compared to longer versions, which can result in the higher promotion of PC12 cell differentiation [45.98]. This means that the cytotoxicity and even the bioeffects of different carbon nanomaterials in vitro are highly dependent on their nanostructures. In more research from our lab, it was shown that anatase TiO_2 particles had a much higher toxicity than rutile ones on the central nervous system [45.99]. The shape of nanoparticles is another important factor that directly affects cellular uptake. For example, it was shown that longer Au nanorods had much less cellular uptake when compared to shorter

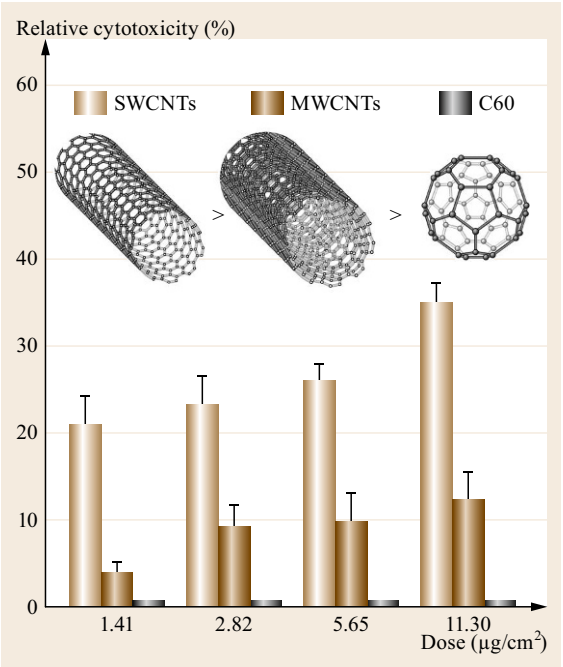

Fig. 45.8 The ranking of cytotoxicity of carbon NMs on a mass basis is: SWCNTs > MWCNTs > C_{60}. Reproduced with permission from reference [45.96]

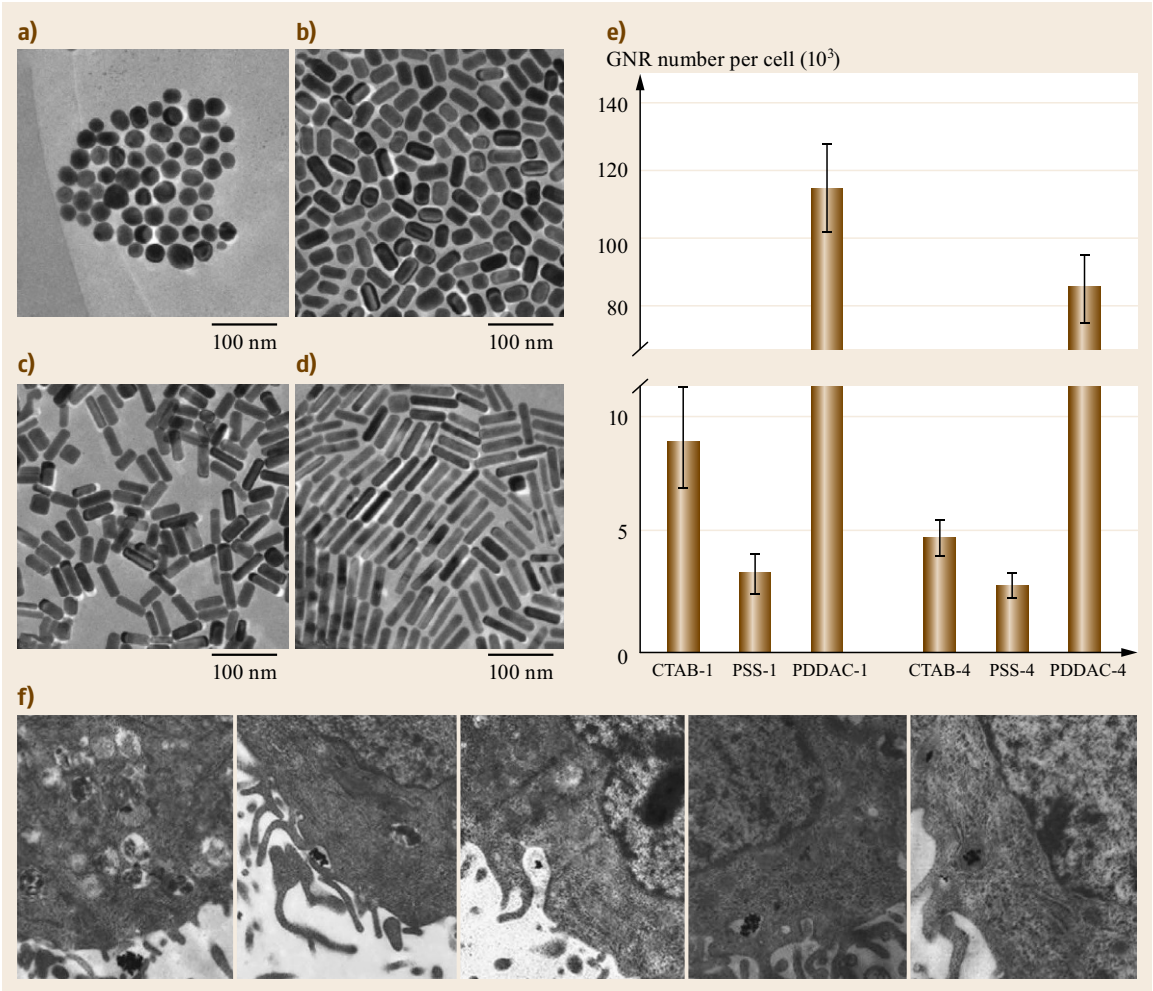

Fig. 45.9a–f Shape and surface-coating determine cellular uptake of Au nanoparticles in Michigan Cancer Foundation-7 (MCF-7) cells. Transmission electron microscope images of CTAB-coated Au nanorods with different aspect ratios: **(a)** CTAB-1, **(b)** CTAB-2, **(c)** CTAB-3, and **(d)** CTAB-4. **(e)** shows the shape- and surface-coating-dependent cellular uptake of Au nanorods coated by CTAB. **(f)** TEM images show the processes of cellular uptake. The Au nanorods form aggregates, enter into vesicles in this form, and move into lysosome. Reproduced from [45.97], with permission from Elsevier

ones, with similar particle surface charges used in the test (Fig. 45.9) [45.24, 97]. Spherical Au nanoparticles entered cells more easily than rod-shaped nanoparticles which may be because a longer membrane wrapping time is required for the rod-shaped particles [45.97].

45.3.3 Agglomeration and Aggregation

NPs have higher surface activity compared to larger sized versions of the same chemical composition. On this basis, the increased surface size also has a strong tendency for agglomeration/aggregation. An agglomeration is a collection of particles that are loosely bound together by relatively weak forces, including van der Waals forces, electrostatic forces, simple physical entanglement, and surface tension, with a resulting external surface area similar to the sum of the surface area of the individual components. Aggregated particles are a cohesive mass consisting of particulate subunits tightly bound by covalent or metallic bonds due to a surface reconstruction, often through melting or annealing of the surface, and often having an external surface area significantly smaller than the sum of the surface areas of the individual components. Agglomerates may be reversible under certain chemical/biological conditions whereas an aggregate

will not easily release primary particles under normal conditions [45.100]. Particulate matter in the air may come from release during the ENM production process. It usually represents a highly complex mixture of particles with different sizes. Field research showed that airborne NMs in occupational settings are mostly 200 to 400 and 2000 to 3000 nm in diameter [45.101, 102]. However, in some special environments such as metal processing, burning, photocopying or printing, and nanomaterial handling processes, the nanopeak of the aerosol is still extremely prominent [45.103–106]. The NMs in the air easily form agglomerates, which influences absorption in the organism after deposition in the inhalation system. The exact deposition dosages of differently sized particles could be estimated by the multiple path particle dosimetry (MPPD) model which was developed for estimating dose in the lower respiratory tract based on particle sizes [45.107, 108]. Toxic effects within the body are usually dominated by the NM agglomeration situation. It has been reported in mice that temporary organ injury occurs in lung and liver due to delayed clearance of agglomerated MWCNTs, while well-dispersed forms were easily eliminated from these organs [45.109]. Similarly, highly agglomerated SWCNTs cause more serious toxic effects on glial cells in both the peripheral nervous system and central nervous system compared with better dispersed SWCNTs [45.110]. In the estimation of the EHS impacts of NMs, the extent of agglomeration/aggregation should be taken into account and thoroughly investigated.

45.3.4 Chemical Composition, Purity, and Impurities

The chemical composition, also defined as elemental composition and chemical structure, is an intrinsic property of all materials. In the development of nanotechnology we see tremendously different NM chemical compositions. Roughly, there are four categories of NMs based on their chemical composition:

1. Carbon nanomaterials (e.g., carbon nanotubes, nanowires, nanocantilevers, graphene, and fullerenes)
2. Metallic and metallic oxide materials (e.g., gold or silver nanoparticles, magnetic nanoparticles, QDs, titanium dioxide, and iron oxide)
3. Silicon nanomaterials (silicon or silica nanoparticles)
4. Organic nanomaterials (e.g., DNA, polymers, polymeric micelles, liposomes, or nanoparticles prepared from polymers or lipids).

Some NMs are a hybrid of different compositions, with the various characteristics used to advantage in the final product. Recently, high content screening (HCS), a cell-based multiparametric image analysis technique, was adopted in the evaluation of eight different compositions of NMs [45.77]. It was found that Ag and ZnO NMs possessed much higher cytotoxicity to 16HBE cells than SiO_2, TiO_2, and CeO_2 based on the same mass level [45.77]. Impurities are inevitable in ENMs, and this needs to be considered when implementing the risk assessment. Raw nanotubes especially those in commercial products usually contain significant impurities, such as inert synthesis supports (silica, alumina) and metal catalysts (iron, cobalt, nickel), derived from the large-scale production procedures, postfabrication and postpurification treatments. Much evidence has shown that the impurities in NMs contribute greatly to increased toxicity through induction of oxidative stress [45.111–113].

45.3.5 Coating, Surface Modification, and Surface Charges

Coating and surface modifications of nanoparticles play an essential role in control of the physicochemical and surface properties of NMs. By employing these techniques, scientists can reduce material toxicity, increase solubility, enhance biocompatibility, and prevent aggregation of NMs in solution or in the air [45.114]. It was indicated that conventional hydrophobic fullerenes and the surface-modified hydrophilic ones have significant differences in terms of toxicity and biological functions [45.115, 116]. We investigated the influence of surface coatings on the cellular uptake and the cytotoxicity of gold nanorods, and found that the cellular uptake of Au NRs is highly dependent on the surface chemistry, as evidenced by poly (diallyldimethyl ammonium chloride) (PPDDAC)-coated Au nanorods exhibiting a much greater ability to be internalized by the cells compared to poly-sodium-*p*-styrenesulfate (PSS) and Cetyltrimethylammonium bromide (CTAB)-coated ones (Fig. 45.9e) [45.97, 117]. In nanotechnology, various nanosynthesis and nanofabrication methods have been applied to the NMs in order to obtain particular characteristics. However, the positive intention of NM modification may lead to unintended side effects, which in turn leads to alarm bells concerning possibly damaging health effects including poor biocompatibility, and acute and chronic toxicity. Surface charge, which can be manipulated by surface modification, is one of the most important factors in relation to the biological functions of nanoparticles. In contrast to neutral and negatively charged nanoparticles, positively charged particles can lead to the most efficient cell membrane penetration and cellular internalization because of their effective binding to negatively charged groups on the cell surface [45.118]. Fluorescent polystyrene (PS) particles

are good research objects to study the intercellular dynamics of allogenic materials in cell models. We investigated the effects of negatively charged carboxylated polystyrene (COOH-PS) and positively charged amino-modified polystyrene (NH_2-PS) nanoparticles with three different diameters (50, 100, and 500 nm) on cancer HeLa cells and normal NIH 3T3 cells during cell cycles. It was disclosed that the PS nanoparticles maintain a distance from the spindle and the chromosomes during the whole mitosis. They were never found to be associated with any components of the mitotic apparatus and no abnormal cell division was detected after their internalization. In addition, no abnormal daughter cells were detected. The data showed that the PS nanoparticles do not influence mitosis which is highly conserved in mammal cells in both normal and cancer cells [45.119].

Besides the aforementioned physicochemical characteristics, there are other factors, as listed in Table 45.2, that may have an influence on toxic impacts on EHS. Because of this situation the toxicity assessment of NMs is usually highly complex with sometimes even fragmentary and contradictory conclusions obtained from various sources [45.120]. Scientists have to face this difficulty and consider characterizing NMs in detail using state-of-the-art nanotechnologies.

45.4 Novel Techniques and Biomarker Development in Nanotoxicology

45.4.1 The Development of Biomarkers for Evaluation of EHS Impacts

The discovery of NM toxicity mechanisms could contribute a series of biomarkers for assessment of EHS impacts. Herein, biomarker is defined as key molecular or cellular events that have a direct link to health outcomes after exposure to NMs. It is highly feasible to fit developed biomarkers with in vitro cell model testing during risk assessment of EHP impacts due to the low costs, lack of an ethical animal abuse issue, and the high-efficiency of testing procedures [45.121]. This is in accordance with the strategy suggested by the US Environmental Protection Agency (EPA) and the National Research Council (NRC): cellular response or adverse outcome pathway (AOP)-based toxicity testing for adverse health effect evaluation should be the preferred toxicity testing strategy in the 21st century [45.122, 123]. Further, the in vitro testing techniques based on the biomakers of AOP generally provide more sensitive hazard identification than those detection methods using the endpoints of toxic effects when considering either the time or dose factors.

For the ENMs most investigated in nanotoxicology research, it is generally accepted that high NM surface area represents high ROS-generating capability which causes oxidative stress in biological systems after nano–bio interactions [45.124]. The high ROS level in the organism leads to the negative effects of the depletion of cellular antioxidants and accumulation of peroxidized lipids [45.25, 125]. In relation to these earlier inducing events, various markers at different tiers can be used in the assessment of EHS impacts of NMs along with the development of toxicity outcomes (Fig. 45.10).

Wang et al. [45.28] showed that MWCNTs could directly activate TGF-β/Smad2 signaling in fibroblasts or epithelial cells with the consequences of inducing the fibroblast-to-myofibroblast transition and EMT, both of which contribute to CNT-induced fibrotic responses. Therefore, it is suggested that TGF-β and the TGF-β receptor signaling system could be considered as potential biomarkers in the risk evaluation of CNTs. Attributed to the same carbon nanomaterial, graphene seems to induce toxicity through a similar mechanism. *Li* et al. [45.126] showed that the signaling pathways of both mitogen-activated protein kinase (MAPK) and TGF-β were activated and resulted in the downstream Bcl-2 protein family initiating mitochondrial-related apoptosis after incubation of the graphene in the RAW 264.7 macrophage cell line. Furthermore, p38 mitogen-activated protein kinase (p38 MAPK), extracellular signal-regulated kinase (ERK), and c-Jun N-terminal kinase (JNK) were significantly upregulated. Similar to the CNT exposure, the stimulated transcription activity of the Smad proteins verified that TGF-β was also found to be activated by graphene. As a result, Bim and Bax were significantly upregulated with the consequences of causing permeabilization of the mitochondrial outer membrane and the release of mitochondrial proapoptotic factors into the cytosol. These results indicate that graphene and CNTs could induce ROS production and trigger the mitochondrial apoptotic pathway, thus leading to apoptosis.

The endoplasmic reticulum (ER) stress and interruption of the aforementioned mitochondria metabolic signaling pathways has been fully investigated in the evaluation of EHS impacts [45.56, 81, 127–131]. ER stress, also known as unfolded protein response (UPR), is an important cellular self-protection mechanism that could be used as an early biomarker for evaluating the toxicity of NMs [45.81]. Toxicity initiates as the adaptation response and ends with toxicity formed after an

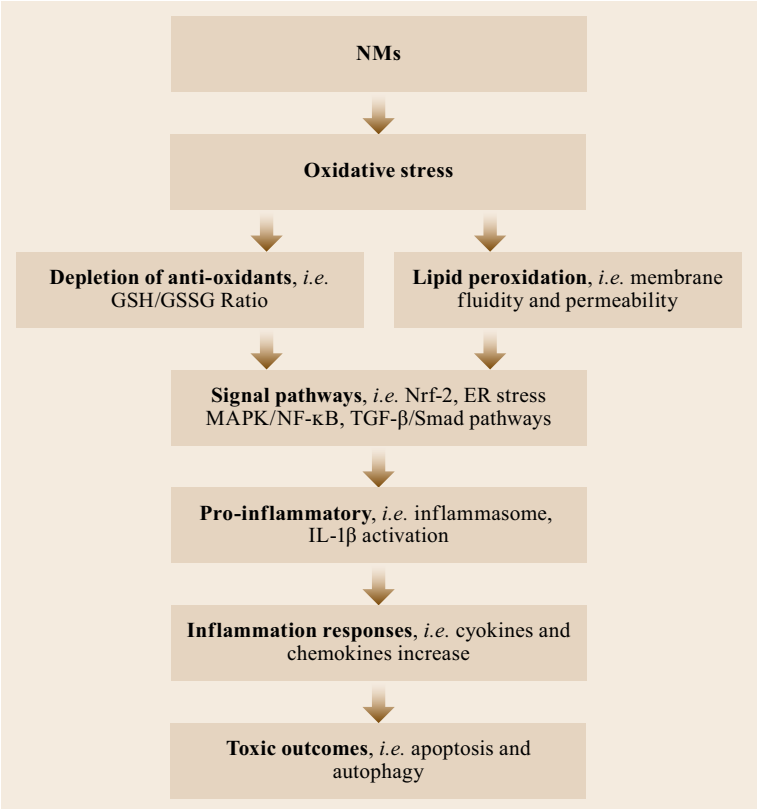

Fig. 45.10 Toxicity mechanisms of NMs and proposed biomarkers in assessment of EHS impacts

exposure dosage higher than the physiological threshold of the cellular self-protection capacity. The ER stress responses contain three dominant stress sensors that include inositol-requiring protein 1 (IRE1), PKR-like endoplasmic reticulum kinase (PERK), and activating transcription factor-6 (ATF-6). The ER-chaperone protein 78 kDa glucose-regulated protein (GRP78), or called binding immunoglobulin protein (BiP), binds these three stress sensors in the normal state, and in its active state releases them when stress occurs. IRE1, which functions as an endoribonuclease, initiates the splicing of x-box binding protein 1 (xbp-1) mRNA after activation. Then, the newly produced spliced form of *xbp-1* (*xbp-1s*) induces the transcription of chaperone protein-encoding genes for self-protection functions (Fig. 45.11). The *xbp-1* splicing and induction of BiP and C/EBP homologous protein (CHOP) have been identified as the specific biomarkers of ER stress responses [45.81, 132]. It is worth noting that ER stress, as a sensitive earlier biomarker, could be used to define the lowest observable effect concentrations (LOEC) in cell and animal models for predesigned safe applications of ENMs [45.77].

High-throughput screening (HTS) techniques and modeling based on QSAR should be developed for analysis of potential EHS hazards from NMs especially when handling NMs with exceedingly variable physicochemical characteristics [45.86, 133]. HTS techniques hold great potential, enabling faster and more reproducible toxicity testing for basic NMs as well as other nanorelated EHS samples. QSAR generally has a close relation to the application of various HTS methods. Therefore, researchers can predict a wide range of properties, including biological activities and toxicities, for new materials using QSAR models; this process depends entirely on the initial input data generated from HTS detection methods. Thus, this predictive toxicological approach will finally aid the design or optimization of NPs with commercially useful properties that are also safe to humans and the environment. Recently, *Le* et al. [45.86] developed QSAR models linking nanoparticle properties to cell viability, membrane integrity, and oxidative stress based on the testing data of 45 types of ZnO nanoparticles with varying particle sizes, aspect ratios, doping types, doping concentrations, and surface coatings. It was found that influencing factors such as the concentrations of NPs the cells are exposed to, the type of surface coating, the nature and extent of doping, and the aspect ratio of the particles provide significant contributions to the cellular toxicity of the NPs. These

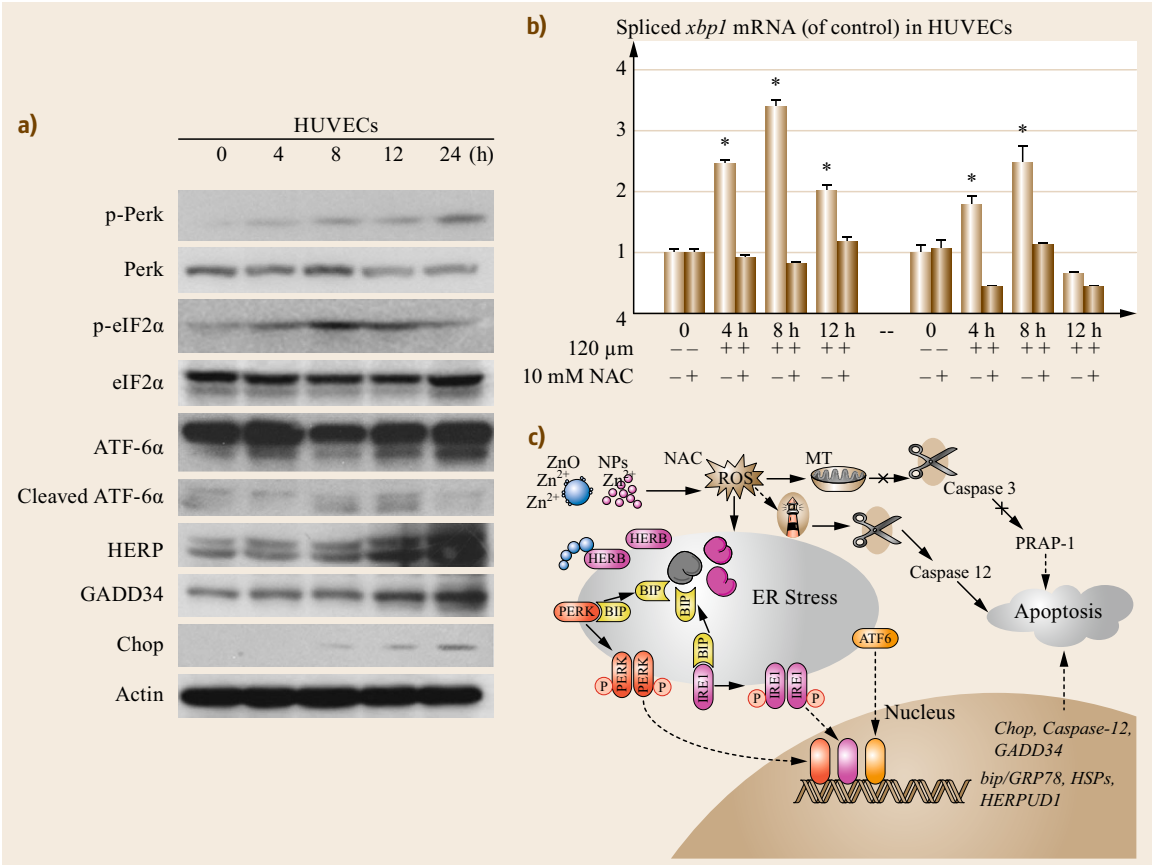

Fig. 45.11 Endoplasmic reticulum (ER) stress is an earlier biomarker for assessment of EHS impacts. **(a)** Western blotting analysis of ER stress-related proteins after exposure in human umbilical vein endothelial cells (HUVEC) at 240 μM. Reprinted with permission from [45.81] copyright 2014 American Chemical Society. **(b)** The PCR detection of spliced *xbp-1* was used for the detection of ER stress response in HUVECs after exposures to ZnO NP and zinc ions. The antioxidant (NAC, *N*-acetyl-cysteine) was used as antioxidant to abolish the ROS accumulation in cells. **(c)** The proposed mechanism for the activation of ER stress pathway after exposure to ZnO NPs

valuable strategies and techniques will promote the development of novel pathway mechanism-based in vitro approaches for assessment of EHS impact of NMs and risk assessment of influences on humans or contamination of ecosystems.

45.4.2 Novel Techniques Used for ADME Study in Nanotoxicology

After they are released and distributed, NMs generally appear as trace elements in biological and environmental science samples. The knowledge about ADME of NMs has high relations to the following evaluations of their EHS impacts. Nuclear analytical techniques (NATs) play important roles in facing the challenges in nanotoxicology [45.134–136]. NATs are a collection of techniques that deal with nuclear excitations, nuclear reactions, electron inner shell excitations, and/or radioactive decay. Typically, they have the advantages of absolute quantification, high sensitivity, excellent accuracy and precision, low matrix effects, and non-destructiveness in analytical applications [45.137, 138]. NATs mostly focus on the analysis of parameters in the samples e.g., nuclear mass, spin and magnetic moment, and excited states. Their application in nanotoxicology have been well summarized in the literature [45.134]. At the molecular level, synchrotron radiation circular dichroism spectroscopy (SRCD), x-ray absorption fine structure (XAFS), circular dichroism spectroscopy (CS), and AFM can be applied to characterize nanomaterials and analyze bio–nano interactions (Fig. 45.12). The cellular visualization of nanoparticles and the study of their transformation within the cell can be achieved through confocal laser scanning mi-

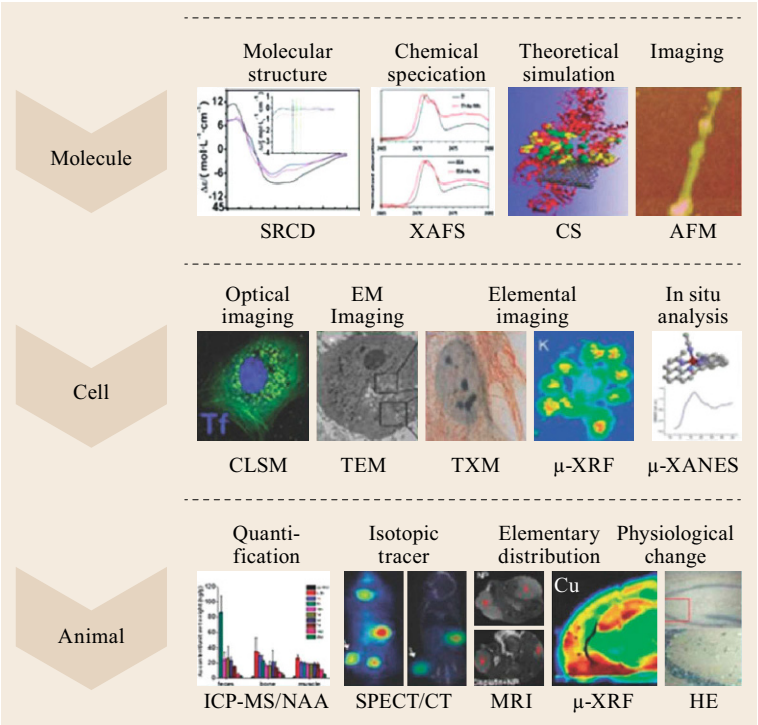

Fig. 45.12 Systematic platform using integrated advanced nuclear techniques for nanotoxicology. Adapted from [45.134] with permission from the Royal Society of Chemistry

croscopy (CLSM), TEM, scanning transmission x-ray microscopy (TXM), x-ray fluorescence (μ-XRF), and x-ray absorption near-edge structure (μ-XANES). Several approaches can execute in vivo ADME analysis: neutron activation analysis (NAA), ICP-MS (inductively coupled plasma mass spectrometry), inductively coupled plasma optical emission spectroscopy (ICP-OES), isotopic tracing (IT), single-photon emission computed tomography (SPECT), positron emission tomography (PET), x-ray computed tomography (CT), magnetic resonance imaging (MRI), fluorescence imaging, and photoacoustic imaging. The NAA, ICP-MS, ICP-OES, and IT techniques require the sacrificing of animals to obtain quantitative information on the NMs. SPECT, PET, x-ray CT, and MRI can show the whole body distribution of nanoparticles directly, while their quantification capabilities are limited. Fluorescence and photoacoustic-based methods have their own unique advantages in some scenarios of in vivo imaging, but the penetration depths are limited due to the limited penetration capability of light and sound compared to x-rays or γ-rays [45.139]. In recent research using the XANES technique, it was disclosed that disulfide bonds in BSA change into Au–S bonds quantitatively on the binding sites of BSA and Au nanorods. At the same time, a stable plane was found for gold–sulfur interaction supported by molecular dynamic simulation [45.140]. Further, the XANES technique has the ability to dissect the chemical transformation of metal NMs in biological systems. For example, it is known that silver NPs can be internalized by cells and degraded inside lysosomes, but how the cytotoxicity developed during the degradation process is unknown. Silver k-edge XANES clearly indicated that intracellular silver can be transformed from elemental Ag to a silver-sulfur (Ag−S−) form which played the dominant role in cytotoxicity [45.141]. XRF imaging is a powerful tool for elemental imaging in biological samples of cells and tissues. It is feasible to combine XRF imaging with XANES for analysis of the same sample. For example, this combined strategy has been used to study the distribution of Se when the worm *C. elegans* engulfs CdSe QDs. XRF imaging showed the locations of accumulation and distribution of Se, while Se k-edge XANES indicated the change in Se chemical forms in different body regions. This combined analysis can provide more accurate information on NMs than the more generally used fluorescence-based optical imaging [45.63]. There are two kinds of TXM, soft x-ray TXM and hard x-ray TXM (Nano-CT). The former can distinguish the NMs and organelles and is suitable for imaging a local region inside a cell due to the small x-ray penetration depth ($\approx 5\,\mu m$) [45.142]. While the latter, Nano-CT, can provide a much wider imaging field in a single cell ($\approx 2-50\,\mu m$) which could be used for three-dimensional (3-D) imaging of the con-

Table 45.3 Nuclear analytical and related techniques for physicochemical characterization, chemical element imaging, quantification, and speciation in nanotoxicological studies. Reproduced with permission from reference [45.134]

Techniques	Exciting radiation	Particle emission	Depth information	Spatial resolution	Detection limit	Chemical structure	Quantitative analysis	Imaging	Materials	Availability	Matrix effects
NAA	Thermal neutrons	Alpha, electrons, neutrons, and x-ray photons	None	None	0.001–0.1 ppm	No	Yes, 2–10%	No	Solids and liquids	Very rare	Less
ICP-MS	Plasma	Ions	None	None	0.00001–10 ppm	Little	Yes, high precision with isotope dilution	No, imaging by LA	Solution	Common	Yes, severe
SIMS	Ions, atoms for FABMS	Secondary ions	3–10 nm	0.02 μm best, 1–5 μm typical	0.1–10 ppm	Some chemical bonds	Yes, to 25% relative error	Yes	Any solid, some liquids	Relatively uncommon	Yes
XRD	x-ray tube or synchrotron x-rays	Diffracted x-rays	None	50 nm–10 μm synchrotron x-rays	1–5% mixtures	Yes, species identity and structure	Yes, to 5–10%	No	Crystalline solids and polymers	Common	Yes
XAS	Synchrotron and some rotating anode x-ray sources	Transmitted or characteristic x-rays	Yes	50 nm synchrotron x-rays	100 ppm	Yes	No	No	Solids and nonvolatile liquids	Rare, at synchrotron facilities	Yes

Table 45.3 (continued)

Techniques	Exciting radiation	Particle emission	Depth information	Spatial resolution	Detection limit	Chemical structure	Quantitative analysis	Imaging	Materials	Availability	Matrix effects
XRF	x-ray tube, synchrotron x-rays	Characteristic x-rays	None	50 nm–10 μm synchrotron x-rays	0.1—10 ppm (≈ synchrotron mg kg^{-1}) x-ray	No	Yes, high precision	Yes	Solids and nonvolatile liquids	XRF common, XRF Mapping only at synchrotron facilities	Yes
EDX	Electron	Characteristic x-ray photons	0.5—5 μm, depends on matrix	2 nm–5 μm, depends on matrix	100–1000 ppm	No	Yes, relative error	No	Any solid	Moderately common	Yes
EELS	Electron	Characteristic electron energy loss		1 nm	1000 ppm	Yes	Yes	No	Any solid	Moderately common	Yes
PIXE	Protons	Characteristic x-ray photons	None	2 μm–20 mm	0.1—10 ppm	No	Yes, 5%	Yes	Any solid	Rare	Yes
Isotopic tracing		Radioactive: α, β, γ-rays and stable isotopes	No		10^{-4}–10^{-8} g	No	Yes	Yes	Any solid	Common	No
PET	Positron	γ-ray	Yes	1 mm	100 ppt	No	Yes	Yes	Any solid	Common	No
SPECT	Single-photon	γ-ray	Yes	1 mm	100 ppt	No	Yes	Yes	Any solid	Common	No

struction of metal NMs [45.141]. Soft x-ray TXM also has its own powerful applications for the analysis of specific elements like Ce in CeO_2 NPs or Gd in Gd-metallofullerenol [45.143, 144]. The characteristics of the whole list of NATs and related techniques are provided in Table 45.3.

45.5 Conclusion and Perspectives

EHS impacts related to nanotechnology were investigated in this chapter. It is obvious that the presence and release of nanoparticles into the environment has important implications for human health and the environment. Scientists should not only focus on the beneficial effects of NPs, but also need to be careful in regard to possible adverse impacts on EHS. Particle attributes such as size, agglomeration or aggregation, composition, structure, coating, and purity are important for the determination of potential impacts on EHS, although they are generally quite complicated. State-of-the-art analysis methods and techniques should be used and developed for the gradually emerging challenges. Such techniques and biomarkers will have meaningful utilization in the protection of human populations, especially in the case of occupational exposure, and in regard to the total ecosystem. As the mechanisms of nanotoxicity and ecotoxicity are still poorly understood, the study of such EHS impacts through NMs definitely needs the input of greater resources. Both researchers and authorities should strive for a sound balance between the development of nanotechnology and the scientific evaluation of EHS impacts in order to achieve a sustainable and harmonious development of nanotechnology.

Acknowledgments. This work was supported by the Ministry of Science and Technology of China (2016YFA0201600), the National Natural Science Foundation of China (21477029, 21320102003, 21277037, 21403043, and 21277080), the Chinese Academy of Sciences (XDA09040400), the Beijing Natural Science Foundation (No. 2152037), Major Project of the National Social Science Fund (Grant No. 12&ZD117) "Ethical issues of high-tech", and the National Science Fund for Distinguished Young Scholars (11425520).

References

45.1 M.H. Hassan: Nanotechnology. Small things and big changes in the developing world, Science **309**, 65–66 (2005)

45.2 K. Donaldson, V. Stone, C.L. Tran, W. Kreyling, P.J. Borm: Nanotoxicology, Occup. Environ. Med. **61**, 727–728 (2004)

45.3 G. Oberdörster, E. Oberdörster, J. Oberdörster: Nanotoxicology: An emerging discipline evolving from studies of ultrafine particles, Environ. Health Perspect. **113**, 823–839 (2005)

45.4 G. Oberdörster: Safety assessment for nanotechnology and nanomedicine: Concepts of nanotoxicology, J. Intern. Med. **267**, 89–105 (2010)

45.5 National Research Council: Health and safety aspects of engineered nanomaterials committee to develop a research strategy for environmental. In: *A Research Strategy for Environmental, Health, and Safety Aspects of Engineered Nanomaterials*, ed. by the Committee to Develop a Research Strategy for Environmental, Health, and Safety Aspects of Engineered Nanomaterials, chaired by J.M. Samet (National Academies, Washington DC 2012)

45.6 C.O. Hendren, X. Mesnard, J. Droge, M.R. Wiesner: Estimating production data for five engineered nanomaterials as a basis for exposure assessment, Environ. Sci. Technol. **45**, 2562–2569 (2011)

45.7 K. Schmid, M. Riediker: Use of nanoparticles in Swiss industry: A targeted survey, Environ. Sci. Technol. **42**, 2253–2260 (2008)

45.8 F. Piccinno, F. Gottschalk, S. Seeger, B. Nowack: Industrial production quantities and uses of ten engineered nanomaterials in Europe and the world, J. Nanopart. Res. **14**, 1–11 (2012)

45.9 N. Li, S. Georas, N. Alexis, P. Fritz, T. Xia, M.A. Williams, E. Horner, A. Nel: A work group report on ultrafine particles (American Academy of Allergy, Asthma & Immunology): Why ambient ultrafine and engineered nanoparticles should receive special attention for possible adverse health outcomes in human subjects, J. Allergy Clin. Immunol. **138**, 386–396 (2016)

45.10 R. Chen, C. Chen: Scenarios in the workplace and risk assessment of carbon nanomaterials. In: *Biomedical Applications and Toxicology of Carbon Nanomaterials*, ed. by C. Chen, H. Wang (Wiley, Weinheim 2016)

45.11 F. Gottschalk, C. Lassen, J. Kjoelholt, F. Christensen, B. Nowack: Modeling flows and concentrations of nine engineered nanomaterials in the Danish environment, Int. J. Env. Res. Public Health **12**, 5581–5602 (2015)

45.12 T.Y. Sun, F. Gottschalk, K. Hungerbühler, B. Nowack: Comprehensive probabilistic modelling of environmental emissions of engineered nanomaterials, Environ. Pollut. **185**, 69–76 (2014)

45.13 Y.S. Tian, F. Gottschalk, K. Hungerbühler, B. Nowack: Comprehensive probabilistic modelling of environmental emissions of engineered nanomaterials, Environ. Pollut. **185**, 69–76 (2014)

45.14 T.Y. Sun, N.A. Bornhoft, K. Hungerbühler, B. Nowack: Dynamic probabilistic modeling of environmental emissions of engineered nanomaterials, Environ. Sci. Technol. **50**, 4701–4711 (2016)

45.15 M. Miseljic, S.I. Olsen: Life-cycle assessment of engineered nanomaterials: A literature review of assessment status, J. Nanopart. Res. **16**, 33 (2014)

45.16 H. Sengul, T.L. Theis, S. Ghosh: Toward sustainable nanoproducts: An overview of nanomanufacturing methods, J. Ind. Ecol. **12**, 329–359 (2008)

45.17 R. Dhingra, S. Naidu, G. Upreti, R. Sawhney: Sustainable nanotechnology: Through green methods and life-cycle thinking, Sustainability **2**, 3323–3338 (2010)

45.18 Y. Ding, T.A. Kuhlbusch, M. Van Tongeren, A.S. Jimenez, I. Tuinman, R. Chen, I.L. Alvarez, U. Mikolajczyk, C. Nickel, J. Meyer, H. Kaminski, W. Wohlleben, B. Stahlmecke, S. Clavaguera, M. Riediker: Airborne engineered nanomaterials in the workplace – A review of release and worker exposure during nanomaterial production and handling processes, J. Hazard. Mater. **322**, 17–28 (2017)

45.19 Y. Zhao, G. Xing, Z. Chai: Nanotoxicology: Are carbon nanotubes safe?, Nat. Nanotechnol. **3**, 191–192 (2008)

45.20 J.C. Bonner: Carbon nanotubes as delivery systems for respiratory disease: Do the dangers outweigh the potential benefits?, Expert. Rev. Respir. Med. **5**, 779–787 (2011)

45.21 C.A. Poland, R. Duffin, I. Kinloch, A. Maynard, W.A. Wallace, A. Seaton, V. Stone, S. Brown, W. Macnee, K. Donaldson: Carbon nanotubes introduced into the abdominal cavity of mice show asbestos-like pathogenicity in a pilot study, Nat. Nanotechnol. **3**, 423–428 (2008)

45.22 P. Wang, X. Nie, Y. Wang, Y. Li, C. Ge, L. Zhang, L. Wang, R. Bai, Z. Chen, Y. Zhao, C. Chen: Multiwall carbon nanotubes mediate macrophage activation and promote pulmonary fibrosis through TGF-beta/Smad signaling pathway, Small **9**, 3799–3811 (2013)

45.23 Y. Liu, Y. Zhao, B. Sun, C. Chen: Understanding the toxicity of carbon nanotubes, Acc. Chem. Res. **46**, 702–713 (2013)

45.24 F. Zhao, Y. Zhao, Y. Liu, X. Chang, C. Chen, Y. Zhao: Cellular uptake, intracellular trafficking and cytotoxicity of nanomaterials, Small **7**, 1322–1337 (2011)

45.25 P. Moller, D.V. Christophersen, D.M. Jensen, A. Kermanizadeh, M. Roursgaard, N.R. Jacobsen, J.G. Hemmingsen, P.H. Danielsen, Y. Cao, K. Jantzen, H. Klingberg, L.G. Hersoug, S. Loft: Role of oxidative stress in carbon nanotube-generated health effects, Arch. Toxicol. **88**, 1939–1964 (2014)

45.26 R. Alshehri, A.M. Ilyas, A. Hasan, A. Arnaout, F. Ahmed, A. Memic: Carbon nanotubes in biomedical applications: Factors, mechanisms and remedies of toxicity, J. Med. Chem. **59**, 8149–8167 (2016)

45.27 Y.Y. Guo, J. Zhang, Y.F. Zheng, J. Yang, X.Q. Zhu: Cytotoxic and genotoxic effects of multi-wall carbon nanotubes on human umbilical vein endothelial cells in vitro, Mutat. Res. **721**, 184–191 (2011)

45.28 P. Wang, Y. Wang, X. Nie, C. Braini, R. Bai, C. Chen: Multiwall carbon nanotubes directly promote fibroblast-myofibroblast and epithelial-mesenchymal transitions through the activation of the TGF-beta/Smad signaling pathway, Small **11**, 446–455 (2015)

45.29 R.R. Mercer, J.F. Scabilloni, A.F. Hubbs, L. Wang, L.A. Battelli, W. McKinney, V. Castranova, D.W. Porter: Extrapulmonary transport of MWCNT following inhalation exposure, Part. Fibre. Toxicol. **10**, 38 (2013)

45.30 K. Donaldson, C.A. Poland, F.A. Murphy, M. MacFarlane, T. Chernova, A. Schinwald: Pulmonary toxicity of carbon nanotubes and asbestos-similarities and differences, Adv. Drug Deliv. Rev. **65**, 2078–2086 (2013)

45.31 M. Sharma, J. Nikota, S. Halappanavar, V. Castranova, B. Rothen-Rutishauser, A.J. Clippinger: Predicting pulmonary fibrosis in humans after exposure to multi-walled carbon nanotubes (MWCNTs), Arch. Toxicol. **90**, 1605–1622 (2016)

45.32 C. Ge, L. Meng, L. Xu, R. Bai, J. Du, L. Zhang, Y. Li, Y. Chang, Y. Zhao, C. Chen: Acute pulmonary and moderate cardiovascular responses of spontaneously hypertensive rats after exposure to single-wall carbon nanotubes, Nanotoxicology **6**, 526–542 (2012)

45.33 I. Huizar, A. Malur, Y.A. Midgette, C. Kukoly, P. Chen, P.C. Ke, R. Podila, A.M. Rao, C.J. Wingard, L. Dobbs, B.P. Barna, M.S. Kavuru, M.J. Thomassen: Novel murine model of chronic granulomatous lung inflammation elicited by carbon nanotubes, Am. J. Respir. Cell Mol. Biol. **45**, 858–866 (2011)

45.34 C.C. Chou, H.Y. Hsiao, Q.S. Hong, C.H. Chen, Y.W. Peng, H.W. Chen, P.C. Yang: Single-walled carbon nanotubes can induce pulmonary injury in mouse model, Nano Lett. **8**, 437–445 (2008)

45.35 R. Chen, L. Zhang, C. Ge, M.T. Tseng, R. Bai, Y. Qu, C. Beer, H. Autrup, C. Chen: Subchronic toxicity and cardiovascular responses in spontaneously hypertensive rats after exposure to multiwalled carbon nanotubes by intratracheal instillation, Chem. Res. Toxicol. **28**, 440–450 (2015)

45.36 T. Ingle, E. Dervishi, A.R. Biris, T. Mustafa, R.A. Buchanan, A.S. Biris: Raman spectroscopy analysis and mapping the biodistribution of inhaled carbon nanotubes in the lungs and blood of mice, J. Appl. Toxicol. **33**, 1044–1052 (2013)

45.37 A.R. Reddy, D.R. Krishna, Y.N. Reddy, V. Himabindu: Translocation and extra pul-

monary toxicities of multi wall carbon nanotubes in rats, Toxicol. Mech. Methods **20**, 267–272 (2010)

45.38 C. Ge, J. Du, L. Zhao, L. Wang, Y. Liu, D. Li, Y. Yang, R. Zhou, Y. Zhao, Z. Chai, C. Chen: Binding of blood proteins to carbon nanotubes reduces cytotoxicity, Proc. Natl. Acad. Sci. USA **108**, 16968–16973 (2011)

45.39 X. Jiang, R. Foldbjerg, T. Miclaus, L. Wang, R. Singh, Y. Hayashi, D. Sutherland, C. Chen, H. Autrup, C. Beer: Multi-platform genotoxicity analysis of silver nanoparticles in the model cell line CHO-K1, Toxicol. Lett. **222**, 55–63 (2013)

45.40 C. Chen, H. Wang: *Biomedical Applications and Toxicology of Carbon Nanomaterials* (Wiley, Weinheim 2016)

45.41 S. Chernousova, M. Epple: Silver as antibacterial agent: Ion, nanoparticle and metal, Angew. Chem. Int. Ed. Engl. **52**, 1636–1653 (2013)

45.42 K. Chaloupka, Y. Malam, A.M. Seifalian: Nanosilver as a new generation of nanoproduct in biomedical applications, Trends Biotechnol **28**, 580–588 (2010)

45.43 C. Lorenz, L. Windler, N. von Goetz, R.P. Lehmann, M. Schuppler, K. Hungerbuhler, M. Heuberger, B. Nowack: Characterization of silver release from commercially available functional (nano) textiles, Chemosphere **89**, 817–824 (2012)

45.44 L. Geranio, M. Heuberger, B. Nowack: The behavior of silver nanotextiles during washing, Environ. Sci. Technol. **43**, 8113–8118 (2009)

45.45 T.M. Benn, P. Westerhoff: Nanoparticle silver released into water from commercially available sock fabrics, Environ. Sci. Technol. **42**, 4133–4139 (2008)

45.46 D.M. Mitrano, E. Rimmele, A. Wichser, R. Erni, M. Height, B. Nowack: Presence of nanoparticles in wash water from conventional silver and nano-silver textiles, ACS Nano **8**, 7208–7219 (2014)

45.47 R. Kaegi, A. Voegelin, C. Ort, B. Sinnet, B. Thalmann, J. Krismer, H. Hagendorfer, M. Elumelu, E. Mueller: Fate and transformation of silver nanoparticles in urban wastewater systems, Water Res **47**, 3866–3877 (2013)

45.48 R. Kaegi, A. Voegelin, B. Sinnet, S. Zuleeg, H. Hagendorfer, M. Burkhardt, H. Siegrist: Behavior of metallic silver nanoparticles in a pilot wastewater treatment plant, Environ. Sci. Technol. **45**, 3902–3908 (2011)

45.49 Y. Yin, J. Liu, G. Jiang: Sunlight-induced reduction of ionic Ag and Au to metallic nanoparticles by dissolved organic matter, ACS Nano **6**, 7910–7919 (2012)

45.50 N. Akaighe, R.I. Maccuspie, D.A. Navarro, D.S. Aga, S. Banerjee, M. Sohn, V.K. Sharma: Humic acid-induced silver nanoparticle formation under environmentally relevant conditions, Environ. Sci. Technol. **45**, 3895–3901 (2011)

45.51 N.F. Adegboyega, V.K. Sharma, K. Siskova, R. Zboril, M. Sohn, B.J. Schultz, S. Banerjee: Interactions of aqueous Ag^{+} with fulvic acids: Mechanisms of silver nanoparticle formation and investigation of stability, Environ. Sci. Technol. **47**, 757–764 (2013)

45.52 D. Lu, Q. Liu, T. Zhang, Y. Cai, Y. Yin, G. Jiang: Stable silver isotope fractionation in the natural transformation process of silver nanoparticles, Nat. Nanotechnol. **11**, 682–686 (2016)

45.53 Y. Li, J.A. Bhalli, W. Ding, J. Yan, M.G. Pearce, R. Sadiq, C.K. Cunningham, M.Y. Jones, W.A. Monroe, P.C. Howard, T. Zhou, T. Chen: Cytotoxicity and genotoxicity assessment of silver nanoparticles in mouse, Nanotoxicology **8**(Suppl 1), 36–45 (2014)

45.54 Z. Wang, G. Qu, L. Su, L. Wang, Z. Yang, J. Jiang, S. Liu, G. Jiang: Evaluation of the biological fate and the transport through biological barriers of nanosilver in mice, Curr. Pharm. Des. **19**, 6691–6697 (2013)

45.55 Y. Zhang, Y. Zhang, G. Hong, W. He, K. Zhou, K. Yang, F. Li, G. Chen, Z. Liu, H. Dai, Q. Wang: Biodistribution, pharmacokinetics and toxicology of Ag_2S near-infrared quantum dots in mice, Biomaterials **34**, 3639–3646 (2013)

45.56 R. Chen, L. Zhao, R. Bai, Y. Liu, L.P. Han, Z.F. Xu, F. Chen, H. Autrup, D.X. Long, C.Y. Chen: Silver nanoparticles induced oxidative and endoplasmic reticulum stresses in mouse tissues: Implications for the development of acute toxicity after intravenous administration, Toxicol. Res. **5**, 602–608 (2016)

45.57 A. Chrastina, J.E. Schnitzer: Iodine-125 radiolabeling of silver nanoparticles for in vivo SPECT imaging, Int. J. Nanomed. **5**, 653–659 (2010)

45.58 D.P. Lankveld, A.G. Oomen, P. Krystek, A. Neigh, A. Troost-de Jong, C.W. Noorlander, J.C. Van Eijkeren, R.E. Geertsma, W.H. De Jong: The kinetics of the tissue distribution of silver nanoparticles of different sizes, Biomaterials **31**, 8350–8361 (2010)

45.59 Y. Xue, S. Zhang, Y. Huang, T. Zhang, X. Liu, Y. Hu, Z. Zhang, M. Tang: Acute toxic effects and gender-related biokinetics of silver nanoparticles following an intravenous injection in mice, J. Appl. Toxicol. **32**, 890–899 (2012)

45.60 Y. Li, T. Qin, T. Ingle, J. Yan, W. He, J.J. Yin, T. Chen: Differential genotoxicity mechanisms of silver nanoparticles and silver ions, Arch. Toxicol. **91**, 509–519 (2017)

45.61 S. Kim, D.Y. Ryu: Silver nanoparticle-induced oxidative stress, genotoxicity and apoptosis in cultured cells and animal tissues, J. Appl. Toxicol. **33**, 78–89 (2013)

45.62 L. Wang, J. Li, J. Pan, X. Jiang, Y. Ji, Y. Li, Y. Qu, Y. Zhao, X. Wu, C. Chen: Revealing the binding structure of the protein corona on gold nanorods using synchrotron radiation-based techniques: understanding the reduced damage in cell membranes, J. Am. Chem. Soc. **135**, 17359–17368 (2013)

45.63 Y. Qu, W. Li, Y. Zhou, X. Liu, L. Zhang, L. Wang, Y.F. Li, A. Iida, Z. Tang, Y. Zhao, Z. Chai, C. Chen: Full assessment of fate and physiological behavior of quantum dots utilizing Caenorhabditis elegans as a model organism, Nano Lett **11**, 3174–3183 (2011)

45.64 X. Jiang, T. Miclaus, L. Wang, R. Foldbjerg, D.S. Sutherland, H. Autrup, C. Chen, C. Beer: Fast intracellular dissolution and persistent cellular uptake of silver nanoparticles in CHO-K1 cells: Im-

plication for cytotoxicity, Nanotoxicology **9**, 181–189 (2015)
45.65 C. Pang, A. Brunelli, C. Zhu, D. Hristozov, Y. Liu, E. Semenzin, W. Wang, W. Tao, J. Liang, A. Marcomini, C. Chen, B. Zhao: Demonstrating approaches to chemically modify the surface of Ag nanoparticles in order to influence their cytotoxicity and biodistribution after single dose acute intravenous administration, Nanotoxicology **10**, 129–139 (2016)
45.66 M. Ahamed, M. Karns, M. Goodson, J. Rowe, S.M. Hussain, J.J. Schlager, Y. Hong: DNA damage response to different surface chemistry of silver nanoparticles in mammalian cells, Toxicol. Appl. Pharmacol. **233**, 404–410 (2008)
45.67 A.K. Suresh, D.A. Pelletier, W. Wang, J.L. Morrell-falvey, B. Gu, M.J. Doktycz: Cytotoxicity induced by engineered silver nanocrystallites is dependent on surface coatings and cell types, Langmuir **28**, 2727–2735 (2012)
45.68 X. Yang, A.P. Gondikas, S.M. Marinakos, M. Auffan, J. Liu, H. Hsu-Kim, J.N. Meyer: Mechanism of silver nanoparticle toxicity is dependent on dissolved silver and surface coating in Caenorhabditis elegans, Environ. Sci. Technol. **46**, 1119–1127 (2012)
45.69 S.R. Saptarshi, A. Duschl, A.L. Lopata: Biological reactivity of zinc oxide nanoparticles with mammalian test systems: An overview, Nanomedicine **10**, 2075–2092 (2015)
45.70 M.J. Osmond, M.J. McCall: Zinc oxide nanoparticles in modern sunscreens: An analysis of potential exposure and hazard, Nanotoxicology **4**, 15–41 (2010)
45.71 B. Gulson, M. McCall, M. Korsch, L. Gomez, P. Casey, Y. Oytam, A. Taylor, M. McCulloch, J. Trotter, L. Kinsley, G. Greenoak: Small amounts of zinc from zinc oxide particles in sunscreens applied outdoors are absorbed through human skin, Toxicol. Sci. **118**, 140–149 (2010)
45.72 T.G. Smijs, S. Pavel: Titanium dioxide and zinc oxide nanoparticles in sunscreens: Focus on their safety and effectiveness, Nanotechnol. Sci. Appl. **4**, 95–112 (2011)
45.73 P. Kelleher, K. Pacheco, L.S. Newman: Inorganic dust pneumonias: The metal-related parenchymal disorders, Environ. Health Perspect. **108**, 685–696 (2000), Suppl 4
45.74 J.M. Fine, T. Gordon, L.C. Chen, P. Kinney, G. Falcone, W.S. Beckett: Metal fume fever: characterization of clinical and plasma IL-6 responses in controlled human exposures to zinc oxide fume at and below the threshold limit value, J. Occup. Environ. Med. **39**, 722–726 (1997)
45.75 W.G. Kuschner, A. D'Alessandro, H. Wong, P.D. Blanc: Early pulmonary cytokine responses to zinc oxide fume inhalation, Environ. Res. **75**, 7–11 (1997)
45.76 H.C. Chuang, H.T. Juan, C.N. Chang, Y.H. Yan, T.H. Yuan, J.S. Wang, H.C. Chen, Y.H. Hwang, C.H. Lee, T.J. Cheng: Cardiopulmonary toxicity of pulmonary exposure to occupationally relevant zinc oxide nanoparticles, Nanotoxicology **8**, 593–604 (2014)
45.77 L. Huo, R. Chen, X. Shi, R. Bai, P. Wang, Y. Chang, C. Chen: High-content screening for assessing nanomaterial toxicity, J. Nanosci. Nanotechnol. **15**, 1143–1149 (2015)
45.78 V. Sharma, P. Singh, A.K. Pandey, A. Dhawan: Induction of oxidative stress, DNA damage and apoptosis in mouse liver after sub-acute oral exposure to zinc oxide nanoparticles, Mutat. Res. **745**, 84–91 (2012)
45.79 J. Wang, X. Deng, F. Zhang, D. Chen, W. Ding: ZnO nanoparticle-induced oxidative stress triggers apoptosis by activating JNK signaling pathway in cultured primary astrocytes, Nanoscale Res. Lett. **9**, 117 (2014)
45.80 V. Sharma, R.K. Shukla, N. Saxena, D. Parmar, M. Das, A. Dhawan: DNA damaging potential of zinc oxide nanoparticles in human epidermal cells, Toxicol. Lett. **185**, 211–218 (2009)
45.81 R. Chen, L. Huo, X. Shi, R. Bai, Z. Zhang, Y. Zhao, Y. Chang, C. Chen: Endoplasmic reticulum stress induced by zinc oxide nanoparticles is an earlier biomarker for nanotoxicological evaluation, ACS Nano **8**, 2562–2574 (2014)
45.82 M. Ramasamy, M. Das, S.S. An, D.K. Yi: Role of surface modification in zinc oxide nanoparticles and its toxicity assessment toward human dermal fibroblast cells, Int. J. Nanomed. **9**, 3707–3718 (2014)
45.83 M. Luo, C. Shen, B.N. Feltis, L.L. Martin, A.E. Hughes, P.F. Wright, T.W. Turney: Reducing ZnO nanoparticle cytotoxicity by surface modification, Nanoscale **6**, 5791–5798 (2014)
45.84 H. Yin, R. Chen, P.S. Casey, P.C. Ke, T.P. Davis, C. Chen: Reducing the cytotoxicity of ZnO nanoparticles by a pre-formed protein corona in a supplemented cell culture medium, RSC Adv **5**, 73963–73973 (2015)
45.85 R. Chen, C. Chen: Nanotoxicity. In: *The Nanobiotechnology Handbook*, ed. by Y. Xie (Taylor Francis, Abingdon 2012) pp. 599–620
45.86 T.C. Le, H. Yin, R. Chen, Y. Chen, L. Zhao, P.S. Casey, C. Chen, D.A. Winkler: An experimental and computational approach to the development of ZnO nanoparticles that are safe by design, Small **12**, 3568–3577 (2016)
45.87 F. Zhao, H. Meng, L. Yan, B. Wang, Y. Zhao: Nanosurface chemistry and dose govern the bioaccumulation and toxicity of carbon nanotubes, metal nanomaterials and quantum dots in vivo, Sci. Bull. **60**, 3–20 (2015)
45.88 H.S. Nalwa, Y. Zhao: *Nanotoxicology* (American Scientific, Stewenson Ranch 2007)
45.89 Z. Chen, H. Meng, G. Xing, C. Chen, Y. Zhao, G. Jia, T. Wang, H. Yuan, C. Ye, F. Zhao, Z. Chai, C. Zhu, X. Fang, B. Ma, L. Wan: Acute toxicological effects of copper nanoparticles in vivo, Toxicol. Lett. **163**, 109–120 (2006)
45.90 Y. Liu, Y. Gao, L. Zhang, T. Wang, J. Wang, F. Jiao, W. Li, Y. Liu, Y. Li, B. Li, Z. Chai, G. Wu, C. Chen: Potential health impact on mice after nasal instillation of nano-sized copper particles and their

translocation in mice, J. Nanosci. Nanotechnol. **9**, 6335–6343 (2009)

45.91 L. Zhang, R. Bai, B. Li, C. Ge, J. Du, Y. Liu, L. Le Guyader, Y. Zhao, Y. Wu, S. He, Y. Ma, C. Chen: Rutile TiO(2) particles exert size and surface coating dependent retention and lesions on the murine brain, Toxicol. Lett. **207**, 73–81 (2011)

45.92 C. Carlson, S.M. Hussain, A.M. Schrand, L.K. Braydich-Stolle, K.L. Hess, R.L. Jones, J.J. Schlager: Unique cellular interaction of silver nanoparticles: size-dependent generation of reactive oxygen species, J. Phys. Chem. B **112**, 13608–13619 (2008)

45.93 J. Rejman, V. Oberle, I. Zuhorn, D. Hoekstra: Size-dependent internalization of particles via the pathways of clathrinand caveolae-mediated endocytosis, Biochem. J. **377**, 159–169 (2004)

45.94 G. Oberdörster, J. Ferin, B.E. Lehnert: Correlation between particle size, in vivo particle persistence and lung injury, Environ. Health Perspect. **102**, 173–179 (1994), Suppl 5

45.95 S. Beg, M. Rizwan, A.M. Sheikh, M.S. Hasnain, K. Anwer, K. Kohli: Advancement in carbon nanotubes: Basics, biomedical applications and toxicity, J. Pharm. Pharmacol. **63**, 141–163 (2011)

45.96 G. Jia, H. Wang, L. Yan, X. Wang, R. Pei, T. Yan, Y. Zhao, X. Guo: Cytotoxicity of carbon nanomaterials: single-wall nanotube, multi-wall nanotube, and fullerene, Environ. Sci. Technol. **39**, 1378–1383 (2005)

45.97 Y. Qiu, Y. Liu, L. Wang, L. Xu, R. Bai, Y. Ji, X. Wu, Y. Zhao, Y. Li, C. Chen: Surface chemistry and aspect ratio mediated cellular uptake of Au nanorods, Biomaterials **31**, 7606–7619 (2010)

45.98 L. Meng, R. Chen, A. Jiang, L. Wang, P. Wang, C.Z. Li, R. Bai, Y. Zhao, H. Autrup, C. Chen: Short multiwall carbon nanotubes promote neuronal differentiation of PC12 cells via up-regulation of the neurotrophin signaling pathway, Small **9**, 1786–1798 (2013)

45.99 J. Wang, Y. Liu, F. Jiao, F. Lao, W. Li, Y. Gu, Y. Li, C. Ge, G. Zhou, B. Li, Y. Zhao, Z. Chai, C. Chen: Time-dependent translocation and potential impairment on central nervous system by intranasally instilled TiO(2) nanoparticles, Toxicology **254**, 82–90 (2008)

45.100 R.A. Yokel, R.C. Macphail: Engineered nanomaterials: Exposures, hazards and risk prevention, J. Occup. Med. Toxicol. **6**, 7 (2011)

45.101 M. Seipenbusch, A. Binder, G. Kasper: Temporal evolution of nanoparticle aerosols in workplace exposure, Ann. Occup. Hyg. **52**, 707–716 (2008)

45.102 D. Brouwer: Exposure to manufactured nanoparticles in different workplaces, Toxicology **269**, 120–127 (2010)

45.103 R. Chen, B. Hu, Y. Liu, J. Xu, G. Yang, D. Xu, C. Chen: Beyond PM2.5: The role of ultrafine particles on adverse health effects of air pollution, Biochim. Biophys. Acta - Gen. Subjects **1860**, 2844–2855 (2016)

45.104 R. Chen, X. Shi, R. Bai, W. Rang, L. Huo, L. Zhao, D. Long, D. Pui, C. Chen: Airborne nanoparticle pollution in a wire electrical discharge machining workshop and potential health risks, Aerosol Air Qual. Res. **15**, 284–294 (2015)

45.105 X. Shi, R. Chen, L. Huo, L. Zhao, R. Bai, D. Long, D.Y. Pui, W. Rang, C. Chen: Evaluation of nanoparticles emitted from printers in a clean chamber, a copy center and office rooms: Health risks of indoor air quality, J. Nanosci. Nanotechnol. **15**, 9554–9564 (2015)

45.106 L.E. Murr, K.F. Soto, K.M. Garza, P.A. Guerrero, F. Martinez, E.V. Esquivel, D.A. Ramirez, Y. Shi, J.J. Bang, J. Venzor III: Combustion-generated nanoparticulates in the El Paso, TX, USA/Juarez, Mexico Metroplex: Their comparative characterization and potential for adverse health effects, Int. J. Environ. Res. Public Health **3**, 48–66 (2006)

45.107 F.R. Cassee, H. Muijser, E. Duistermaat, J.J. Freijer, K.B. Geerse, J.C. Marijnissen, J.H. Arts: Particle size-dependent total mass deposition in lungs determines inhalation toxicity of cadmium chloride aerosols in rats. Application of a multiple path dosimetry model, Arch. Toxicol. **76**, 277–286 (2002)

45.108 S. Anjilvel, B. Asgharian: A multiple-path model of particle deposition in the rat lung, Fundam. Appl. Toxicol. **28**, 41–50 (1995)

45.109 M.M. Methner, M.E. Birch, D.E. Evans, B.K. Ku, K. Crouch, M.D. Hoover: Identification and characterization of potential sources of worker exposure to carbon nanofibers during polymer composite laboratory operations, J. Occup. Environ. Hyg. **4**, D125–130 (2007)

45.110 L. Belyanskaya, S. Weigel, C. Hirsch, U. Tobler, H.F. Krug, P. Wick: Effects of carbon nanotubes on primary neurons and glial cells, Neurotoxicology **30**, 702–711 (2009)

45.111 K. Pulskamp, S. Diabate, H.F. Krug: Carbon nanotubes show no sign of acute toxicity but induce intracellular reactive oxygen species in dependence on contaminants, Toxicol. Lett. **168**, 58–74 (2007)

45.112 C. Ge, W. Li, Y. Li, B. Li, J. Du, Y. Qiu, Y. Liu, Y. Gao, Z. Chai, C. Chen: Significance and systematic analysis of metallic impurities of carbon nanotubes produced by different manufacturers, J. Nanosci. Nanotechnol. **11**, 2389–2397 (2011)

45.113 L. Meng, A. Jiang, R. Chen, C.Z. Li, L. Wang, Y. Qu, P. Wang, Y. Zhao, C. Chen: Inhibitory effects of multiwall carbon nanotubes with high iron impurity on viability and neuronal differentiation in cultured PC12 cells, Toxicology **313**, 49–58 (2013)

45.114 G. Zeng, G. Wang, F. Guan, K. Chang, H. Jiao, W. Gao, S. Xi, B. Yang: Human amniotic membrane-derived mesenchymal stem cells labeled with superparamagnetic iron oxide nanoparticles: the effect on neuron-like differentiation in vitro, Mol. Cell Biochem. **357**, 331–341 (2011)

45.115 J.J. Yin, F. Lao, P.P. Fu, W.G. Wamer, Y. Zhao, P.C. Wang, Y. Qiu, B. Sun, G. Xing, J. Dong, X.J. Liang, C. Chen: The scavenging of reactive oxygen species and the potential for cell protection by functionalized fullerene materials, Bio-

materials **30**, 611–621 (2009)
45.116 Y. Liu, F. Jiao, Y. Qiu, W. Li, F. Lao, G. Zhou, B. Sun, G. Xing, J. Dong, Y. Zhao, Z. Chai, C. Chen: The effect of $Gd@C_{82}(OH)_{22}$ nanoparticles on the release of Th1/Th2 cytokines and induction of TNF-alpha mediated cellular immunity, Biomaterials **30**, 3934–3945 (2009)
45.117 L. Wang, Y.F. Li, L. Zhou, Y. Liu, L. Meng, K. Zhang, X. Wu, L. Zhang, B. Li, C. Chen: Characterization of gold nanorods in vivo by integrated analytical techniques: Their uptake, retention, and chemical forms, Anal. Bioanal. Chem. **396**, 1105–1114 (2010)
45.118 R.R. Arvizo, O.R. Miranda, M.A. Thompson, C.M. Pabelick, R. Bhattacharya, J.D. Robertson, V.M. Rotello, Y.S. Prakash, P. Mukherjee: Effect of nanoparticle surface charge at the plasma membrane and beyond, Nano Lett **10**, 2543–2548 (2010)
45.119 Y. Liu, W. Li, F. Lao, Y. Liu, L. Wang, R. Bai, Y. Zhao, C. Chen: Intracellular dynamics of cationic and anionic polystyrene nanoparticles without direct interaction with mitotic spindle and chromosomes, Biomaterials **32**, 8291–8303 (2011)
45.120 H.F. Krug: Nanosafety research–are we on the right track?, Angew. Chem. Int. Ed. Engl. **53**, 12304–12319 (2014)
45.121 H. Thomas: Toxicology for the twenty-first century, Nature **460**, 208–212 (2009)
45.122 M. Firestone, R. Kavlock, H. Zenick, M. Kramer, U.E.W.G.F. Toxicity: The US environmental protection agency strategic plan for evaluating the toxicity of chemicals, J. Toxicol. Environ. Health B Crit. Rev. **13**, 139–162 (2010)
45.123 D. Krewski, D. Acosta Jr., M. Andersen, H. Anderson, J.C. Bailar III, K. Boekelheide, R. Brent, G. Charnley, V.G. Cheung, S. Green Jr., K.T. Kelsey, N.I. Kerkvliet, A.A. Li, L. McCray, O. Meyer, R.D. Patterson, W. Pennie, R.A. Scala, G.M. Solomon, M. Stephens, J. Yager, L. Zeise: Toxicity testing in the 21st century: A vision and a strategy, J. Toxicol. Environ. Health B Crit. Rev. **13**, 51–138 (2010)
45.124 A. Nel, T. Xia, L. Madler, N. Li: Toxic potential of materials at the nanolevel, Science **311**, 622–627 (2006)
45.125 L. Wang, Y. Min, D. Xu, F. Yu, W. Zhou, A. Cuschieri: Membrane lipid peroxidation by the peroxidase-like activity of magnetite nanoparticles, Chem. Commun. **50**, 11147–11150 (2014)
45.126 Y. Li, Y. Liu, Y. Fu, T. Wei, L.L. Guyader, G. Gao, R.S. Liu, Y.Z. Chang, C. Chen: The triggering of apoptosis in macrophages by pristine graphene through the MAPK and TGF-beta signaling pathways, Biomaterials **33**, 402–411 (2012)
45.127 L. Huo, R. Chen, L. Zhao, X. Shi, R. Bai, D. Long, F. Chen, Y. Zhao, Y.Z. Chang, C. Chen: Silver nanoparticles activate endoplasmic reticulum stress signaling pathway in cell and mouse models: The role in toxicity evaluation, Biomaterials **61**, 307–315 (2015)
45.128 R. Chen, D. Ling, L. Zhao, S. Wang, Y. Liu, R. Bai, S. Baik, Y. Zhao, C. Chen, T. Hyeon: Parallel comparative studies on mouse toxicity of oxide nanoparticle- and gadolinium-based T1 MRI contrast agents, ACS Nano **9**, 12425–12435 (2015)
45.129 H. Yuan, Q. Zhang, J. Guo, T. Zhang, J. Zhao, J. Li, A. White, P.L. Carmichael, C. Westmoreland, S. Peng: A PGC-1alpha-mediated transcriptional network maintains mitochondrial redox and bioenergetic homeostasis against doxorubicin-induced toxicity in human cardiomyocytes: Implementation of TT21C, Toxicol. Sci. **150**, 400–417 (2016)
45.130 H. James, N. Sashi, S. Rachel, C. Conn, K. Sinead, W. Yvonne: A high-throughput dual parameter assay for assessing drug-induced mitochondrial dysfunction provides additional predictivity over two established mitochondrial toxicity assays, Toxicol. Vitro **27**, 560–569 (2012)
45.131 J. Xu, M. Han, Y. Ren, J. Li: The principle of compromise in competition: Exploring stability condition of protein folding, Sci. Bull. **60**, 76–85 (2015)
45.132 A. van Schadewijk: E.F. van't Wout, J. Stolk, P.S. Hiemstra: A quantitative method for detection of spliced x-box binding protein-1 (XBP1) mRNA as a measure of endoplasmic reticulum (ER) stress, Cell Stress Chaperones **17**, 275–279 (2012)
45.133 A. Nel, T. Xia, H. Meng, X. Wang, S. Lin, Z. Ji, H. Zhang: Nanomaterial toxicity testing in the 21st century: Use of a predictive toxicological approach and high-throughput screening, Acc. Chem. Res. **46**, 607–621 (2013)
45.134 C. Chen, Y.F. Li, Y. Qu, Z. Chai, Y. Zhao: Advanced nuclear analytical and related techniques for the growing challenges in nanotoxicology, Chem. Soc. Rev. **42**, 8266–8303 (2013)
45.135 Z. Chai, X. Mao, Z. Hu, Z. Zhang, C. Chen, W. Feng, S. Hu, H. Ouyang: Overview of the methodology of nuclear analytical techniques for speciation studies of trace elements in the biological and environmental sciences, Anal. Bioanal. Chem. **372**, 407–411 (2002)
45.136 L. Wang, C. Chen: Pathophysiologic mechanisms of biomedical nanomaterials, Toxicol. Appl. Pharm. **299**, 30–40 (2016)
45.137 Y.F. Li, C. Chen, A. Bai, S. Li, Q. Wang, J. Wang, Y. Gao, Y. Zhao, Z. Chai: Simultaneous speciation of selenium and mercury in human urine samples from long-term mercury-exposed populations with supplementation of selenium-enriched yeast by HPLC-ICP-MS, J. Anal. At. Spectrom. **22**, 925–930 (2007)
45.138 C. Chen, Z. Chai, Y. Gao: *Nuclear Analytical Techniques for Metallomics and Metalloproteomics* (RSC, Cambridge 2010)
45.139 D. Chen, W. Chao, N. Xin, S. Li, R. Li, M. Guan, L. Zhuang, C. Chen, C. Wang, C. Shu: Photoacoustic imaging guided near-infrared photothermal therapy using highly water-dispersible single-walled carbon nanohorns as theranostic agents, Adv. Funct. Mater. **24**, 6621–6628 (2014)
45.140 L. Wang, J. Li, J. Pan, X. Jiang, Y. Ji, Y. Li, Y. Qu, Y. Zhao, X. Wu, C. Chen: Revealing the binding structure of the protein corona on gold nanorods

using synchrotron radiation-based techniques: Understanding the reduced damage in cell membranes, J. Am. Chem. Soc. **135**, 17359–17368 (2013)

45.141 L. Wang, T. Zhang, P. Li, W. Huang, J. Tang, P. Wang, J. Liu, Q. Yuan, R. Bai, B. Li, K. Zhang, Y. Zhao, C. Chen: Use of synchrotron radiation-analytical techniques to reveal chemical origin of silver-nanoparticle cytotoxicity, ACS Nano **9**, 6532–6547 (2015)

45.142 D. Drescher, P. Guttmann, T. Büchner, S. Werner, G. Laube, A. Hornemann, B. Tarek, G. Schneider, J. Kneipp: Specific biomolecule corona is associated with ring-shaped organization of silver nanoparticles in cells, Nanoscale **5**, 9193–9198 (2013)

45.143 P. Zhang, Y. Ma, Z. Zhang, X. He, J. Zhang, Z. Guo, R. Tai, Y. Zhao, Z. Chai: Biotransformation of ceria nanoparticles in cucumber plants, ACS Nano **6**, 9943–9950 (2012)

45.144 Z. Chen, L. Ying, B. Sun, L. Han, J. Dong, L. Zhang, L. Wang, W. Peng, Y. Zhao, C. Chen: Polyhydroxylated metallofullerenols stimulate IL-1β secretion of macrophage through TLRs/MyD88/NF-κB pathway and NLRP3 inflammasome activation, Small **10**, 2362–2372 (2014)